Original Research Article

Pulmonary Circulation

Revisiting the mechanism of hypoxic pulmonary vasoconstriction using isolated perfused/ventilated mouse lung

Pritesh P. Jain[1], Susumu Hosokawa[1,2], Mingmei Xiong[1,3], Aleksandra Babicheva[1], Tengteng Zhao[1], Marisela Rodriguez[1], Shamin Rahimi[1], Kiana Pourhashemi[1], Francesca Balistrieri[1], Ning Lai[1], Atul Malhotra[1], John Y.-J. Shyy[4], Daniela Valdez-Jasso[5], Patricia A. Thistlethwaite[6], Ayako Makino[7] and Jason X.-J. Yuan[1]

[1]Section of Physiology, Division of Pulmonary, Critical Care and Sleep Medicine, University of California, San Diego, CA, USA; [2]Department of Pediatrics, Tokyo Medical and Dental University, Tokyo, Japan; [3]Department of Critical Medicine, The Third Affiliated Hospital of Guangzhou Medical University, Guangzhou, China; [4]Division of Cardiovascular Medicine, Department of Medicine, University of California, San Diego, USA; [5]Department of Bioengineering, University of California, San Diego, CA, USA; [6]Department of Surgery, University of California, San Diego, CA, USA; [7]Division of Endocrinology and Metabolism, University of California, San Diego, CA, USA

Abstract

Hypoxic Pulmonary Vasoconstriction (HPV) is an important physiological mechanism of the lungs that matches perfusion to ventilation thus maximizing O_2 saturation of the venous blood within the lungs. This study emphasizes on principal pathways in the initiation and modulation of hypoxic pulmonary vasoconstriction with a primary focus on the role of Ca^{2+} signaling and Ca^{2+} influx pathways in hypoxic pulmonary vasoconstriction. We used an ex vivo model, isolated perfused/ventilated mouse lung to evaluate hypoxic pulmonary vasoconstriction. Alveolar hypoxia (utilizing a mini ventilator) rapidly and reversibly increased pulmonary arterial pressure due to hypoxic pulmonary vasoconstriction in the isolated perfused/ventilated lung. By applying specific inhibitors for different membrane receptors and ion channels through intrapulmonary perfusion solution in isolated lung, we were able to define the targeted receptors and channels that regulate hypoxic pulmonary vasoconstriction. We show that extracellular Ca^{2+} or Ca^{2+} influx through various Ca^{2+}-permeable channels in the plasma membrane is required for hypoxic pulmonary vasoconstriction. Removal of extracellular Ca^{2+} abolished hypoxic pulmonary vasoconstriction, while blockade of L-type voltage-dependent Ca^{2+} channels (with nifedipine), non-selective cation channels (with 30 μM SKF-96365), and TRPC6/TRPV1 channels (with 1 μM SAR-7334 and 30 μM capsazepine, respectively) significantly and reversibly inhibited hypoxic pulmonary vasoconstriction. Furthermore, blockers of Ca^{2+}-sensing receptors (by 30 μM NPS2143, an allosteric Ca^{2+}-sensing receptors inhibitor) and Notch (by 30 μM DAPT, a γ-secretase inhibitor) also attenuated hypoxic pulmonary vasoconstriction. These data indicate that Ca^{2+} influx in pulmonary arterial smooth muscle cells through voltage-dependent, receptor-operated, and store-operated Ca^{2+} entry pathways all contribute to initiation of hypoxic pulmonary vasoconstriction. The extracellular Ca^{2+}-mediated activation of Ca^{2+}-sensing receptors and the cell–cell interaction via Notch ligands and receptors contribute to the regulation of hypoxic pulmonary vasoconstriction.

Keywords

alveolar hypoxia, calcium ion, isolated mouse lung, L-type Ca^{2+} channel, transient receptor potential channel

Date received: 31 March 2020; accepted: 16 August 2020

Pulmonary Circulation 2020; 10(4) 1–18
DOI: 10.1177/2045894020956592

Introduction

Acute alveolar hypoxia causes pulmonary vasoconstriction, whereas acute hypoxemia causes systemic (e.g. coronary) vasodilation.[1] Hypoxic pulmonary vasoconstriction (HPV) is

Corresponding author:
Jason X.-J. Yuan, Section of Physiology, Division of Pulmonary, Critical Care and Sleep Medicine, Department of Medicine, MC 0856 University of California, San Diego 9500, Gilman Drive La Jolla, CA 92093-0856, USA.
Email: jxyuan@health.ucsd.edu

an important physiological mechanism for matching perfusion with ventilation, which ensures the maximal oxygenation of the venous blood in pulmonary artery (PA). HPV is a unique or intrinsic feature of the pulmonary vasculature.[2] Although HPV has been extensively studied,[3] the exact cellular and molecular mechanisms still remain unclear. Pulmonary vasoconstriction, similar to systemic vasoconstriction, is caused by pulmonary vascular smooth muscle contraction.[4] An increase in cytosolic free Ca^{2+} concentration ($[Ca^{2+}]_{cyt}$) in pulmonary arterial smooth muscle cells (PASMCs) is a major trigger for pulmonary vasoconstriction. Removal or chelation of extracellular Ca^{2+} significantly inhibits agonist- and high K^+-induced vasoconstriction in isolated PA rings,[5,6] indicating that Ca^{2+} influx through various Ca^{2+}-permeable cation channels in the plasma membrane of PASMCs is required for pulmonary vasoconstriction.

One of the early proposed mechanisms of HPV is triggered by hypoxia-induced blockade of K^+ channels in PASMCs, which induces membrane depolarization and subsequently the opening of voltage-dependent Ca^{2+} channels (VDCC) in the plasma membrane.[6,7] Ca^{2+} influx through VDCC results in a rise in $[Ca^{2+}]_{cyt}$ that triggers PASMC contraction and ultimately pulmonary vasoconstriction.[8] Pharmacological blockade of VDCC using, for example, verapamil and nifedipine (Nif), significantly inhibits HPV but fails to abolish HPV,[5,9] while blockers of VDCC abolish the high K^+-induced pulmonary vasoconstriction.[10–13] These observations suggest that Ca^{2+} influx through cation channels other than VDCC, such as receptor-operated Ca^{2+} channels (ROC) and store-operated Ca^{2+} channels (SOC), are also involved in initial increases in $[Ca^{2+}]_{cyt}$ in PASMC which trigger HPV.[9,14]

There are six subtypes of VDCC based on functional characteristics and biophysical properties, including L-type, T-type, N-type, P-type, Q-type, and R-type VDCC.[15] The high voltage-activated and slowly inactivating L-type VDCC have been substantially studied in vascular smooth muscle cells including PASMC. They are believed to play an important role in increasing $[Ca^{2+}]_{cyt}$ in PASMC during hypoxia.[16] L-type VDCC is also highly expressed in other types of cells such as neuron, cardiomyocytes, skeletal muscle cells, fibroblast, and kidney cells.[17] The low voltage-activated and rapidly inactivating T-type VDCC is implicated in the regulation of vascular smooth muscle cell proliferation,[18] but their potential role in HPV is unclear. In addition to VDCC, there are multiple voltage-independent Ca^{2+}-permeable channels that are responsible for agonist- and growth factor-induced increases in $[Ca^{2+}]_{cyt}$ in PASMC.[19–21] Activation of G protein-coupled receptor (GPCR), for instance, ROC formed by transient receptor potential (TRP) channels and SOC formed by Stromal interaction molecule (STIM) and Orai/TRP, are both involved in inducing increases in $[Ca^{2+}]_{cyt}$ required for stimulating cell contraction, migration, and proliferation.[22,23] Multiple GPCRs,[24] such as Ca^{2+}-sensing receptors (CaSR),[20] muscarinic receptors (M_1),[25,26] and endothelin receptors (ET_A/ET_B)[27] and their ligands are implicated in the development and progression of pulmonary hypertension (PH). We have shown that CaSR contributes partially to acute HPV.[20] ET_A receptor mediates the HPV through inhibition of ATP-sensitive K^+ channels in isolated rat lungs and intact animals.[28] Furthermore, endothelin-1 induces pulmonary vasoconstriction through ET_A receptor via phospholipase and inositol triphosphate (IP_3) and diacylglycerol (DAG) pathways.[29] There is substantial evidence that hypoxia stimulates many different signaling cascades and pathways to increase $[Ca^{2+}]_{cyt}$ in PASMC. It has been demonstrated that hypoxia induces Ca^{2+} release from the intracellular stores such as sarcoplasmic reticulum (SR).[30] Apart from Ca^{2+} influx through Ca^{2+}-permeable cation channels and Ca^{2+} mobilization from intracellular stores, activation of Rho-kinase signaling may also be involved in HPV.[31,32]

In this study, we used an isolated perfused/ventilated mouse lung model and pharmacological approaches to examine potential involvement of various membrane receptors and ion channels in HPV. The isolated perfused/ventilated lung preparation is a widely used ex vivo model to study mechanisms of HPV because it has no influence from central and peripheral nervous system and the systemic circulation, while the preparation includes the intact whole lungs that are ventilated by a mini-ventilator to emulate alveolar ventilation and superfused by an automatic pump to emulate pulmonary vascular perfusion.[5,33,34] Although we focused on using isolated perfused/ventilated lung preparation in this study, we have to note that other preparations and experimental models, such as intact animals, isolated pulmonary arterial rings, and isolated PASMC,[35–40] are all useful preparations for studying mechanisms of HPV.[3,41] The advantage of using the isolated perfused/ventilated lung to study HPV is that (*i*) it reflects the functional changes of the whole lung vasculature, (*ii*) it introduces alveolar hypoxia via ventilation to the vasculature, (*iii*) it allows to superfuse inhibitors into PA or the whole pulmonary vasculature via a perfusion pump to examine their effect; (*iv*) it shows very similar time-course and pharmacological properties shown in intact animals and human subjects; (*v*) it also minimizes the impact of other organs and nervous systems on HPV while maintaining the intact lung in a relatively physiological setting (e.g. consistently ventilated and perfused); and (*vi*) it allows us to examine whether genetic deletion or overexpression of certain genes affect HPV. Here, we aimed at utilizing the isolated perfused/perfused mouse lung model to revisit the mechanisms involved in HPV by focusing on Ca^{2+} signaling and its regulation.

Materials and methods

Isolated perfused/ventilated mouse lung

C57BL/6 mice (approximately 25 g body weight, male, 8–10 weeks old) were used in this study, and the animal experimental protocol was approved by the Institutional Animal

Care and Use Committee (IACUC) at The University of Arizona, Tucson, and University of California, San Diego. The background of *trpc6*$^{-/-}$ (stock #37345) and *notch3*$^{-/-}$ (stock # 010547) mice is C57Bl/6 mice and initial breeding pairs were obtained from Jackson's Laboratory.[42,43]

Mice were anesthetized by pentobarbital sodium (120 mg/kg) via intraperitoneal injection. After tracheostomy, isolated lungs were immediately ventilated with normoxic gas mixture of 21% O_2/5% CO_2 using a rodent ventilator (Minivent type 845, Harvard Apparatus, USA). The respiration rate was maintained at 80 breaths/min with a tidal volume of approximately 250 µl. Positive end expiratory pressure was maintained at 2 cmH_2O. End inspiratory pressure was measured by a pressure transducer (MPX type 399/2, Hugo Sachs Elektronik-Harvard Apparatus, Germany) connected to a tracheal catheter. The mice were placed in an isolated lung open perfusion system chamber (IL-1 Type 839, Harvard Apparatus, USA) with a heated water jacket at 37°C. After tracheal intubation, the chest was opened by median sternotomy and thymus and adipose tissue were carefully excised. Heparin (20 IU) was immediately injected into the right ventricle to prevent blood from coagulation.

A catheter was inserted into the main PA via the right ventricle, which was ligated together with ascending aorta using a 6-0 black silk suture. The PA catheter was connected with a pressure sensor (P75 Type 379, Hugo Sachs Elektronik-Harvard Apparatus, Germany) that was used to continuously measure pulmonary arterial pressure (PAP). Another catheter was inserted into the left atrium via a small incision of the left ventricle (LV) to allow perfusate to drain to reservoir. The pulmonary flow rate was set and maintained at 1 ml/min by a peristaltic pump (ISM 834, ISOMATEC, USA). The Powerlab data acquisition system (AD Instruments, CO, USA) was used to store and analyze the imaging data.

Physiological salt solution (PSS) or saline was occasionally applied to the isolated lungs to moisten the lung tissue. The lung vasculature was consistently superfused with PSS via a pump while the lung airway and alveoli were ventilated with normoxic or hypoxic gas. Raising extracellular [K^+] from 4.7 mM to 40 mM in PSS causes membrane depolarization in PASMC and pulmonary vasoconstriction due to a shift of the equilibrium potential for K^+ from –85 mV to −31 mV. Before experimentation, the isolated lungs were first superfused with the 40 mM K^+-containing PSS (40 K), at least three times, to stabilize the basal PAP and the amplitudes of 40 K-induced increases in PAP. When the basal PAP was stabilized, the lungs were repetitively challenged by ventilation of hypoxic gas (1% O_2 in N_2, for 4 min) to induce an increase in PAP due to alveolar hypoxia-induced pulmonary vasoconstriction (HPV). In the interval of hypoxic challenges, the lungs were ventilated with normoxic gas (21% O_2 in N_2). Pharmacological effects of various ion channel blockers and membrane receptor inhibitors on HPV were examined by superfusion of PSS containing each of the inhibitors with prior treatment for up to 10 min before the lungs were ventilated with hypoxic gas. We do not have direct experimental data showing the optimal time for the maximal inhibition of inhibitors used in the study.

The following inhibitors and blockers were used in this study: (*i*) the blockers of VDCC, Nifedipine (Nif) (0.1 µM, for blocking L-type channels),[5] TTA-A2 (30 µM, for blocking T-type channels),[44] and conotoxin (CoTX) (1 µM, for blocking P/Q type channels)[45]; (*ii*) the inhibitors of Ca^{2+}-activated chloride (Cl^-) channels, N-((4-methoxy)-2-naphthyl)-5-nitroanthranilic acid (MONNA or MON, 10 µM, for blocking TMEM16A/anoctamin-1 channels), and CaCCinh-A01 (10 µM, also for blocking TMEM16A/anoctamin-1 channels)[46]; (*iii*) the inhibitors of non-selective cation channels and TRP channels, SKF-96365 (30 µM, for blocking TRP canonical (TRPC) channels), SAR-7334 (1 µM, for blocking TRPC6 channels),[47] capsazepine (CPZ) (30 µM, for blocking TRP vanilloid 1 (TRPV1) channels),[48] benzamil (Ben) (10 µM, for blocking TRP polycystic (TRPP) channels),[49] AM0902 (10 µM, for blocking TRPA channels),[50] and gadolinium (Gd^{3+}, 10 µM for blocking TRP mucolipin (TRPML) channels)[51,52]; (i*v*) the inhibitor of Notch signaling pathway, (2 *S*)-*N*-[(3,5-Difluorophenyl)acetyl]-L-alanyl-2-phenyl]glycine 1,1-dimethylethyl ester (DAPT, 30 µM, for inhibiting γ-secretase)[43]; and (*v*) the inhibitors of membrane receptors, NPS2143 (30 µM, for blocking extracellular calcium-sensing receptors/CaSR),[20,53] tropicamide (TRO) (10 µM, for blocking muscarinic receptors),[54] and BQ-123 (10 µM, for blocking endothelin receptor A).[28] The concentrations of various drugs used in this study were based on previously published literature. Table 1 lists all the inhibitors (and their targets) used in this study.

Experimental mouse model of PH

C57BL/6 mice (approximately 25 g body weight, male, 8–10 weeks old) were used in this study, and the animal experimental protocol was approved by the IACUC at The University of Arizona, Tucson, and our University. C57Bl/6 J mice were exposed to normobaric hypoxia (10%) in a well-ventilated chamber for four weeks to induce PH. The hypoxia chamber had an oxygen sensor (ProOx P110-E702) which continuously monitored the oxygen levels. Following hypoxic exposure, mice were continuously anesthetized under inhaled isoflurane (1.5%). Right ventricle systolic pressure was measured by right heart catheterization using a pressure catheter (Millar Instruments, PVR1030, 1 F, 4 E, 3 mm, 4.5 cm, Colorado, USA) introduced via right jugular vein. Data were recorded and analyzed using Lab Chart Pro1.0 software (AD Instruments).

Lung angiography

Mice were anesthetized by intraperitoneal injection of pentobarbital sodium (120 mg/kg), and then heparin

Table 1. Inhibitors and drugs used in the study.

Inhibitors	Abbreviations	Target
Nifedipine	Nif	L-type of voltage-dependent Ca^{2+} channel
2-(4-Cyclopropylphenyl)-N-[(1R)-1-[5-(2,2,2-trifluoroethoxy)pyridin-2-yl]ethyl]acetamide (TTA-A2)	TTA-A2	T-type of voltage-dependent Ca^{2+} channel
Conotoxin	CoTX	P/Q-type of voltage-dependent Ca^{2+} channel
SKF-96365	SKF	Transient receptor potential (TRP) canonical (C) channels
4-[[(1R,2R)-2-[(3R)-3-amino-1-piperidinyl]-2,3-dihydro-1H-inden-1-yl]oxy]-3-chlorobenzonitrile dihydrochloride (SAR-7334)	SAR	TRPC6 channels
CPZ	CPZ	TRPV1 channels
Benzamil	Benzamil	TRPP channels
1-[[3-[2-(4-Chlorophenyl)ethyl]-1,2,4-oxadiazol-5-yl]methyl]-1,7-dihydro-7-methyl-6H-purin-6-one (AM 0902)	AM 0902	TRPA channels
Gadolinium	Gd^{3+}	TRPML channels
2-Chloro-6-[(2R)-3-[[1,1-dimethyl-2-(2-naphthalenyl)ethyl]amino-2-hydroxypropoxy]benzonitrile hydrochloride (NPS 2143)	NPS	Calcium sensing receptor
TRO	TRO	Muscarinic M4 receptor
Cyclo (D-Trp-D-Asp-Pro-D-Val-Leu) (BQ-123)	BQ-123	Endothelin A receptor
N-[N-(3,5-Difluorophenacetyl)-L-alanyl]-S-phenylglycine t-butyl Ester (DAPT)	DAPT	γ-secretase (indirect inhibitor of Notch)
2-[(4-Methoxy-2-naphthalenyl)amino]-5-nitro-benzoic acid (MONNA)	MONNA	TMEM16A subunit of calcium activated chloride channel
6-(1,1-Dimethylethyl)-2-[(2-furanylcarbonyl)amino]-4,5,6,7-tetrahydrobenzo[b]thiophene-3-carboxylic acid (CaCCinh-A01)	A01	Ca^{2+}-activated Cl^- channel

(20 IU) was injected immediately into the heart to prevent blood from clotting. A polyethylene (PE-20) tube was cannulated into the PA via the right ventricle; and phosphate-buffered saline was perfused through the PA using an automated pump (NE-300, Pump Systems, for 3 min at a speed of 0.05 ml/min). Then, 0.08 ml of microfil polymer (yellow) (FlowTech Inc., Carver, MA) was perfused into the PA at a speed of 0.05 ml/min. Then, the microfil polymer-filled lungs were kept at 4°C overnight. The next day, the lungs were dehydrated using different concentrations of ethanol: once in 50%, 70%, 80%, and 95% ethanol, and twice in 99.9% ethanol. After dehydration, the lungs were placed in methyl salicylate (Sigma Aldrich, USA) at room temperature on a shaker for overnight in order to show only the vasculature. Lungs were then photographed or imaged with a digital camera (MU1000, FMA050, Amscope, CA). The peripheral lung vascular image, covering the peripheral area of the lung, 1 mm width from the edge was selected with Photoshop CS software, and the branches on the images in Photoshop were outlined manually and later converted to binary images with NIH Image J 1.8v software for quantitative analysis. The total length of branches, the number of branches, and the number of junctions on the skeletonized images were obtained by Image J software and were normalized by the area selected within the peripheral regions of the lung.

Western blot

Lung tissues harvested from mice were homogenized with radioimmunoprecipitation (RIPA) buffer, followed by protein isolation. The samples were diluted with 6 × SDS-sample buffer (Boston BioProducts, USA), heated for 10 min at 95°C, and loaded on 10% SDS polyacrylamide gels. The protein samples were separated by electrophoresis and transferred to a 0.45 µm nitrocellulose membrane (BioRad, USA). The membrane was blocked with 5% bovine serum albumin (Sigma) in Tris-Buffered Saline with Tween 20 (TTBS) for an hour at room temperature and then incubated overnight at 4°C with anti-Notch3 (VMA00484, 1:1000, Bio-Rad) or anti-TRPC6 (bs-2393R, 1:1000, Bioss) primary monoclonal antibody. The membrane was washed with 1X Tris-Buffered Saline, 0.1% Tween® 20 Detergent (TBST) and then incubated for an hour at room temperature with the secondary anti-mouse or anti-rabbit IgG, Horseradish peroxidase (HRP)-linked antibody (1:5000; Cell Signaling). The membrane was subsequently developed after adding substrate (Thermo Fisher Scientific). All membranes were probed for Pan-Actin antibody (Cat# 4968S, 1:2000, Cell Signaling) or β-actin antibody (Cat# sc-47778, 1:1500, Santa Cruz Biotechnology) as internal controls. Band intensities on the membrane were quantified using Image J software.

Solutions and chemicals

The composition of PSS (perfusate) consisted of 120 mM NaCl, 4.3 mM KCl, 1.8 mM $CaCl_2$, 1.2 mM $MgCl_2$, 19 mM $NaHCO_3$, 1.1 mM KH_2PO_4, 10 mM glucose, and 20% fetal bovine serum (pH 7.4). To block endogenous prostaglandin synthesis, 3.1 μM sodium meclofenamate was added to the perfusate. High-K^+ solution (or 40 mM K^+ solution) was prepared by replacing NaCl with equimolar KCl (40 mM). Ca^{2+}-free (0Ca) solution was prepared by replacing $CaCl_2$ with equimolar $MgCl_2$ with 1 mM EGTA added to chelate the residual Ca^{2+}. Mg^{2+}-free (0 Mg) solution was prepared by replacing $MgCl_2$ with equimolar NaCl. Nif, CPZ, AM-0902, CaCCinh, MONNA, Ben, TTA-A2, BQ-123, or TRO was dissolved in DMSO to make a stock solution and aliquoted for storage at –20°C. SKF-96335, SAR-7334, Gd^{3+}, or CoTX was dissolved in water to make a stock solution and aliquoted for storage at –20°C. Aliquots were diluted into final PSS right before the time the inhibitor-containing PSS was perfused into the isolated lungs via the right ventricle.

Statistical analysis

The composite data are shown as mean ± standard error (SEM). Paired or unpaired Student's *t*-test and one way analysis of variance (ANOVA) with Bonferroni multiple comparison test were used for statistical analysis. *p* Value <0.05 was considered as statistically significant.

Results

As shown in pulmonary angiogram, the mouse lungs are composed of a single large lobe on the left side (insert Fig. 1Aa) and four small lobes in the right side (insert Fig. 1Ab). The angiography images of the left and right lungs clearly demonstrate the vascular complexity and density of the pulmonary vascular tree. The highly organized branching pattern is shown from the left and right extrapulmonary arteries to peripheral pulmonary vasculature in all lobes of both sides (Insert Fig. 1Aa and Ab, upper panels). Inspection of the lung periphery region (1 mm width from the edge) at high magnification reveals large numbers of

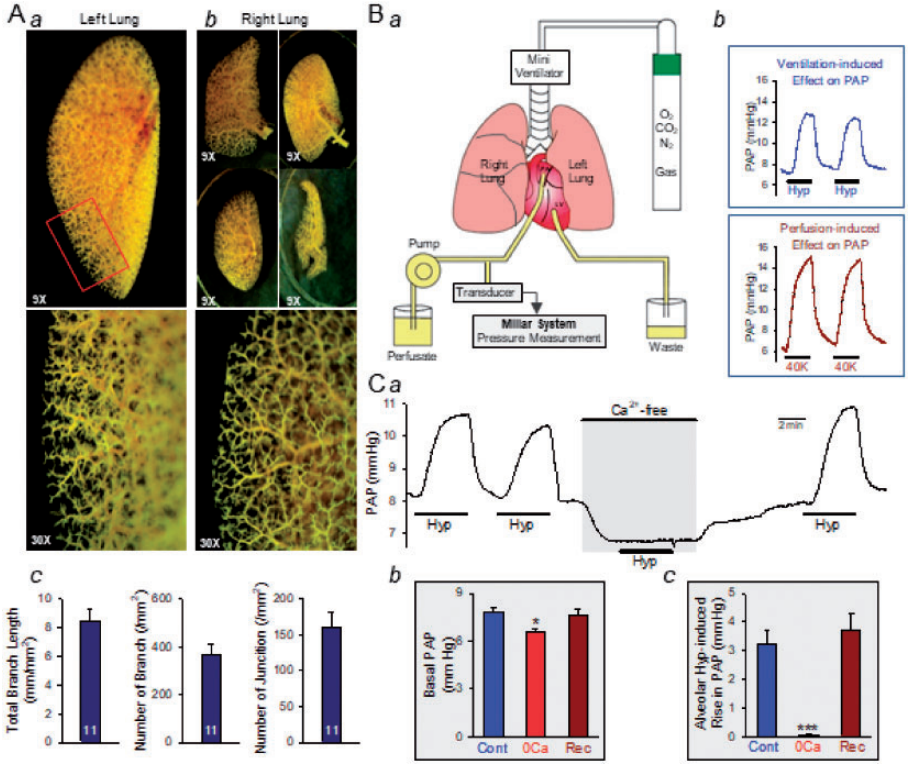

Fig. 1. Removal of extracellular Ca^{2+} decreases the basal pulmonary arterial pressure (PAP) and abolishes the acute hypoxia-induced increase in PAP in isolated perfused/ventilated mouse lungs. (A) Representative lung angiograph of the left lung (a) and right lung lobes (b) from a C57/BL6 mouse. Summarized data (c, means ± SE) showing the total branch length, number of branch, and number of junctions of the left lung vasculature per square millimeter of area ($n = 11$ mouse lungs). (B) Schematic diagram (a) of the isolated perfused/ventilated lung preparation and representative records (b) of pulmonary arterial pressure (PAP) in the lungs ventilated with hypoxic gas (1% O_2 in N_2) by tracheal intubation (upper insert) or perfused with high-K^+ solution through a right ventricular/pulmonary arterial catheter (lower insert). (C) Representative record (a) of PAP before, during, and after ventilation with hypoxic gas (Hyp, (1% O_2 in N_2 for 4 min) when the lung was perfused with physiological salt solution (PSS) with or without (Ca^{2+}-free) 1.8 mM extracellular Ca^{2+}. Summarized data (means ± SE, $n = 6$ mouse lungs) showing the basal PAP and the acute hypoxia-induced increases in PAP before (Cont), during (0Ca), and after (Rec) the lungs are superfused with Ca^{2+}-free (0Ca) PSS. $^{***}p < 0.001$, $^{*}p < 0.05$ vs. Cont (blue) and Rec (dark red) bars.

vascular branches and junctions (Insert Fig. 1Aa and Ab, lower panels). As shown in Fig. 1Ac, the total length of branches, the number of branches, and the number of junctions at a given area (1 mm^2) are 8.5 ± 0.8 mm, 366.4 ± 42.6, and 161.1 ± 20.9 ($n = 11$), respectively, at the peripheral regions of the left lung (insert Fig. 1Ac).

For measuring PAP in the open perfusion isolated perfused/ventilated lung, we used (*i*) a mini pump to consistently superfuse PSS into PA via right ventricle and (*ii*) a mini ventilator to ventilate room air (normoxic control, 21% O_2) into the airway and alveoli (insert Fig. 1Ba). PAP was measured by a pressure transducer and recorded by Power Lab (AD Instruments) via a catheter connected to the perfusion tube (Fig. 1Ba). By ventilating hypoxic gas mixture (1% O_2, 5% CO_2 in N2), we were able to observe a significant increase in PAP due to HPV (Fig. 1Bb, upper inset). By perfusing high-K^+ PSS, we were able to observe an increase in PAP due to 40 mM K^+-induced pulmonary vasoconstriction (Fig. 1Bb, lower inset). By perfusing PSS containing a vasoconstrictive agonist, we were able to observe an increase in PAP due to agonist-induced pulmonary vasoconstriction (data not shown). The amplitude of PAP increase during four minutes of alveolar hypoxia was at the range of 3–5 mmHg (insert Fig. 1C), while the amplitude of 40 mM K^+-induced increase in PAP was around 6–9 mmHg.

HPV is dependent on extracellular Ca^{2+} influx

Removal of extracellular Ca^{2+} in the perfusate (Ca^{2+}-free) or PSS significantly decreased the basal PAP and abolished the alveolar hypoxia-induced increase in PAP due to HPV (insert Fig. 1Ca). Upon restoration of extracellular [Ca^{2+}] to 1.8 mM, the basal PAP returned to control level (insert Fig. 1Cb) and the hypoxia-induced increase in PAP (insert Fig. 1Cc) was also fully recovered (insert Fig. 1Ca–c). These results indicate that extracellular Ca^{2+} is not only necessary for maintaining basal PAP, but also required for alveolar hypoxia-induced increase in PAP due to HPV. The 20% decrease in basal PAP and the 90% inhibition of HPV when the pulmonary vasculature was superfused with Ca^{2+}-free PSS indicate that Ca^{2+} influx through Ca^{2+}-permeable cation channels in PASMC plays an important role in the regulation of pulmonary vascular reactivity and HPV.

HPV is dependent on Ca^{2+} influx through L-type of VDCC

In the next set of experiment, we aimed to identify specific VDCC that contribute to HPV in mouse lung using selective blockers for different types of VDCC. Superfusion of Nif (0.1 μM), a L-type VDCC blocker, significantly and reversibly inhibited alveolar hypoxia-induced increases in PAP due to HPV (insert Fig. 2a). Intrapulmonary perfusion of TTA-A2 (30 μM), a specific blocker of T-type VDCC slightly decreased the basal PAP but had negligible effect on alveolar hypoxia-induced increase in PAP (insert Fig. 2b). CoTX (1 μM), by selectively blocking P/Q-type VDCC, had no effect on the basal PAP and the amplitude of alveolar hypoxia-induced increase in PAP (insert Fig. 2c). These results indicate that Ca^{2+} influx through, at least, L-type VDCC is involved in alveolar hypoxia-induced increase in PAP due to HPV.

HPV is dependent on Ca^{2+} influx through TRP-formed non-selective cation channels

TRP channels have been demonstrated to form ROC[55,56] and SOC.[57,58] To determine specific TRP channels involved in HPV in mouse lung, we used selective blockers for different TRP isoforms in the next set of pharmacological experiments. As shown in Fig. 3, intrapulmonary arterial superfusion of SKF-96365 (SKF, 30 μM) (insert Fig. 3a), a blocker of TRPC channels,[59] and SAR-7334 (SAR, 1 μM) (insert Fig. 3b), a specific blocker of TRPC6 channels,[47] had no obvious effect on the basal PAP, but significantly and reversibly inhibited alveolar hypoxia-induced increases in PAP. Blockade of TRPV1 channel by CPZ (30 μM) also exerted significant and reversible inhibitory effect on alveolar hypoxia-induced increases in PAP or HPV (insert Fig. 3c), whereas selective blockers for TRPP channels, Ben (10 μM), TRPA channels, AM0902 (AM, 10 μM) and TRPML channels, Gd^{3+} (10 μM) negligibly affected HPV or alveolar hypoxia-induced increases in PAP (insert Fig. 3d–f). Consistent with the pharmacological experiments using TRPC6 blocker SAR-7334 (insert Fig. 3b) and TRPC blocker SKF-96365 (insert Fig. 3a), genetic deletion of the *TRPC6* gene (insert Fig. 3g) significantly inhibited HPV in isolated mouse lungs (insert Fig. 3h). The amplitude of alveolar hypoxia-induced increase in PAP in isolated perfused/ventilated lungs from *trpc6*$^{-/-}$ mice was similar to that in isolated lungs from wild-type (WT) mice when the lungs were superfused with PSS containing the TRPC blocker SKF-96365 or the TRPC6 blocker SAR-7334 (insert Fig. 3g and Fig. 3a and b). These results led us to conclude that TRPC channels (especially the TRPC6 channel) and TRPV channels (e.g. TRPV1) are involved in acute hypoxia-induced Ca^{2+} influx and increases in $[Ca^{2+}]_{cyt}$ in PASMC that triggers HPV.

Regulation of HPV by CaSR, a GPCR

CaSR, ET_A and M_4 receptors are three GPCRs expressed in PASMC, which are activated by extracellular Ca^{2+},[20] endothelin-1 (ET-1)[60] and acetylcholine (ACh),[61] respectively. It has been demonstrated that activation of these receptors induce Ca^{2+} influx through ROC and SOC, thus increasing $[Ca^{2+}]_{cyt}$ in PASMCs.[20] As shown in Fig. 4, intrapulmonary arterial perfusion of NPS2143 (30 μM), an allosteric blocker of CaSR, significantly and reversibly inhibited alveolar hypoxia-induced increase in PAP (insert Fig. 4a). However, neither TRO (10 μM), a specific M4 receptor blocker, nor BQ-123 (10 μM), a selective ET_A receptor

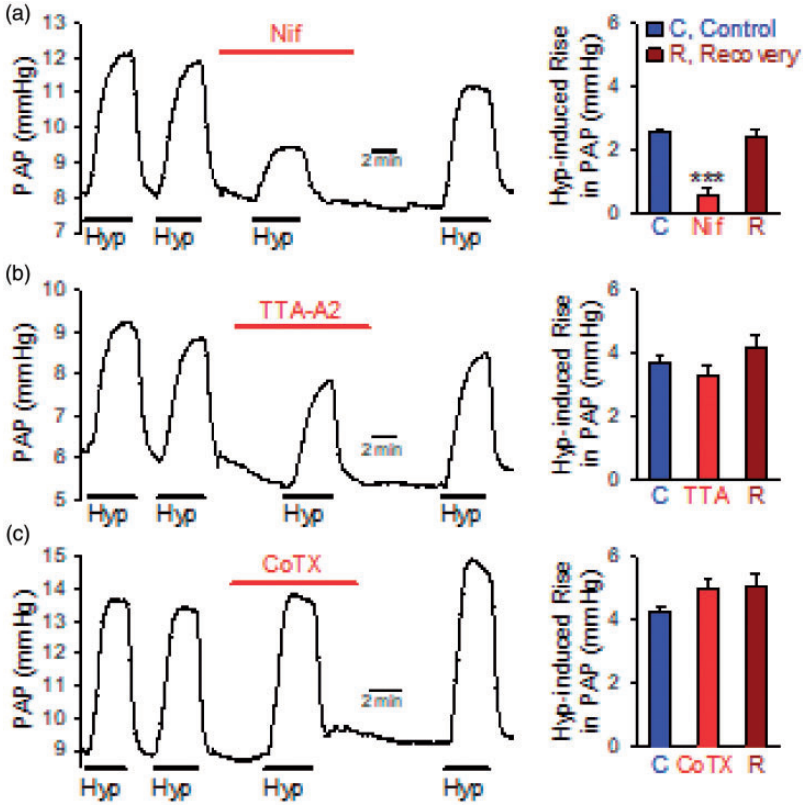

Fig. 2. Blockade of L-type of voltage-dependent Ca^{2+} channels (VDCC) significantly inhibits hypoxia-induced increase in pulmonary arterial pressure (PAP) in isolated perfused/ventilated mouse lungs. (a–c) Representative records (left panels) showing changes of pulmonary arterial pressure (PAP) induced by ventilation of hypoxic gas (1% O_2 for 4 min) before, during, and after perfusion of nifedipine (Nif, 0.1 μM, a L-type VDCC blocker, (a), TTA-A2 (30 μM, a T-type VDCC blocker, (b) or ϖ-Conotoxin (CoTX, 1 μM, an N, P/Q-type VDCC blocker, (c). Summarized data (means ± SE, right panels, $n = 6$ mouse lungs) showing the acute hypoxia-induced increases in PAP before (Control), during, and after (Recovery) perfusion with PSS containing Nif (a), TTA-A2 (b), or CoTX (c). ***$p < 0.001$ vs Control (c, blue) bars and Recovery (R, dark red) bars.

blocker, exerted any effect on alveolar hypoxia-induced increase in PAP or HPV (insert Fig. 4b and c). These results indicate that activation of CaSR is involved in mediating or modulating acute alveolar hypoxia-induced pulmonary vasoconstriction by priming ROC and SOC.[20]

Regulation of HPV by notch signaling pathway

Notch signaling has been implicated in lung vascular development,[62] upregulated Notch ligands (e.g. Jaged-1), and Notch receptors (e.g. Notch1 and Notch3) have been linked to concentric pulmonary vascular remodeling and occlusive intimal lesions in patients with PAH.[42,43,63] Acute superfusion of DAPT (30 μM), a γ-secretase inhibitor that blocks Notch signaling in signal-receiving cells,[43] significantly and reversibly diminished the amplitude of alveolar hypoxia-induced increase in PAP due to HPV (insert Fig. 5a). The 50% reduction of acute HPV by DAPT (insert Fig. 5a, right panel) implied that rapid cleavage of Notch receptors or formation of Notch intracellular domain (NICD) was involved in HPV by, directly or indirectly, modulating hypoxia-induced increase in $[Ca^{2+}]_{cyt}$ in PASMC. Furthermore, in isolated perfused/ventilated lungs from *notch3*$^{-/-}$ mice (insert Fig. 5b), the amplitude of alveolar hypoxia-induced increase in PAP was approximately 45% less than that in isolated lungs from the WT littermates (insert Fig. 5c). These data indicate that Notch3, a Notch receptor that is predominantly expressed in vascular smooth muscle cells, might be involved in regulation of HPV.

HPV is not affected by Ca^{2+}-activated Cl^- channel activity

Intracellular or cytosolic Cl^- concentration ($[Cl^-]_{cyt}$) is very high in smooth muscle cells[64]; the estimated $[Cl^-]_{cyt}$ in vascular smooth muscle cells is in the range of 30–50 mM.[65–67] Due to the high $[Cl^-]_{cyt}$, the equilibrium potential of Cl^- is thus less negative than the resting membrane potential in smooth muscle cells like PASMC. Accordingly, activation of Cl^- channel, such as Ca^{2+}-activated Cl^- (Cl_{Ca}) channels, in PASMC would result in inward currents (or Cl^- efflux) and therefore membrane depolarization, which may subsequently activate VDCC, induce Ca^{2+} influx, and increase $[Ca^{2+}]_{cyt}$ in PASMC. Intrapulmonary arterial superfusion of CaCCinh-A01 (A01, 10 μM), a specific blocker of Cl_{Ca}

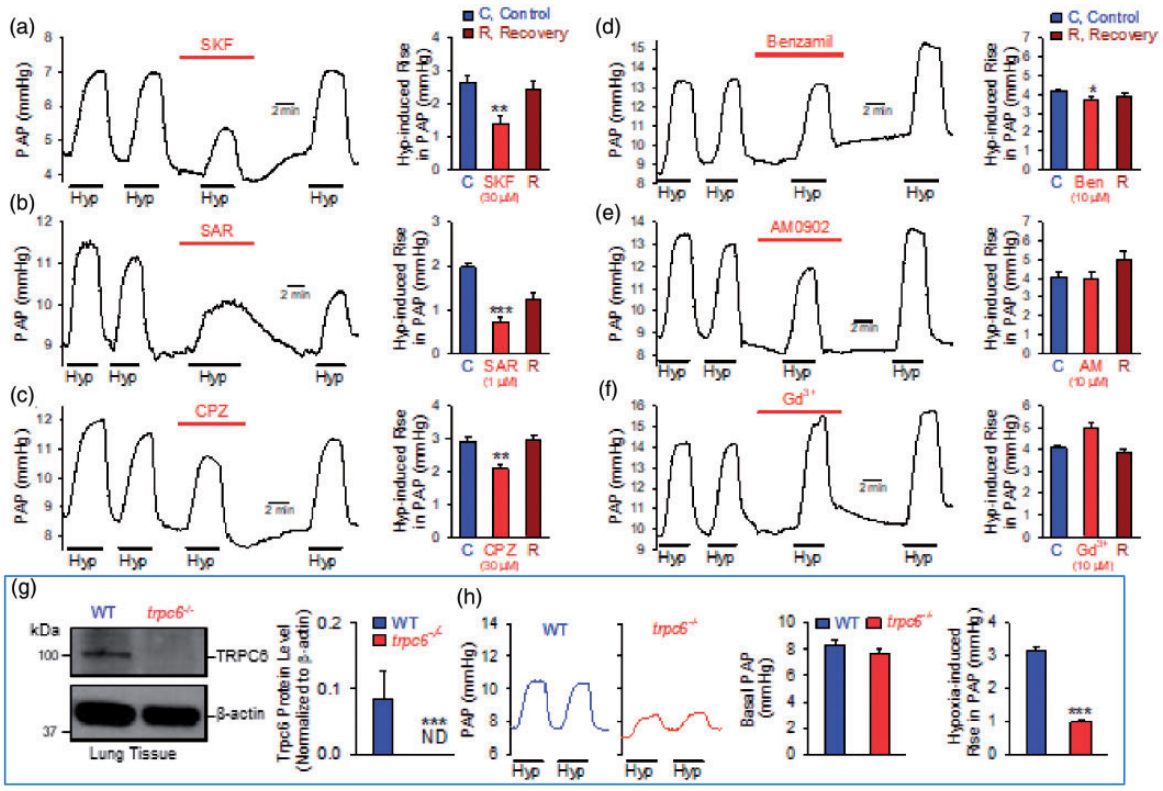

Fig. 3. Blockade of transient receptor potential (TRP) channels significantly inhibits the acute hypoxia-induced increase in pulmonary arterial pressure (PAP) in isolated perfused/ventilated mouse lungs. (a–f) Representative records (left panels) showing changes of PAP induced by ventilation of hypoxic gas (1% O_2 in N_2 for 4 min) before, during, and after perfusion of SKF 96365 (SKF, 30 μM, a TRPC channel blocker, a), SAR-7334 (SAR, 1 μM, a TRPC6 channel blocker, b), capsazepine (CPZ, 30 μM, a TRPV1 channel blocker, c), benzamil (Ben, 10 μM, a TRPP3 channel blocker, d), AM0902 (AM, 10 μM, a TRPA channel blocker, e), or gadolinium (Gd^{3+}, 10 μM, a TRPML channel blocker, f). Summarized data (means ± SE, right panels, $n = 6$ mouse lungs) showing the hypoxia-induced increases in PAP before (Control), during, and after (Recovery) perfusion with PSS containing SKF, SAR, CPZ, Ben, AM, or Gd^{3+}, respectively. $^{**}p < 0.01$, $^{*}p < 0.05$ vs. control (Cont, blue) bars. (g) Representative Western blot image (left panel) and summarized data (means ± SE, right panel, $n = 3$ independent experiments from five mice) of TRPC6 in whole lung tissues from wild-type (WT) and Trpc6 knock-out (*trpc6*$^{-/-}$) mice. $^{***}p < 0.001$ vs. WT. (h) Representative records (left panels) showing changes of PAP when the lungs from WT and *trpc6*$^{-/-}$ mice are ventilated with normoxic (21% O_2 in N_2) and hypoxic (1% O_2 in N_2, for 4 min) gas. Summarized data (means ± SE, $n = 5$ mouse lungs) showing basal PAP (middle panel) and acute hypoxia-induced rises in PAP (right panel) in isolated lungs from WT (blue) and *trpc6*$^{-/-}$ (red) mice. $^{***}p < 0.001$ vs WT.
ND: not detectable.

channels, and MONNA (MO, 10 μM), a specific blocker of TMEM16A which forms Cl_{Ca} channel, had no effect on HPV or alveolar hypoxia-induced increases in PAP (insert Fig. 6a and b). These results indicate that activation of Ca^{2+}-activated Cl^- channels, such as TMEM16A, are not involved in the alveolar hypoxia-induced pulmonary vasoconstriction. The Ca^{2+}-induced membrane depolarization due to activation of Cl_{Ca} channels during hypoxia may be compromised by the Ca^{2+}-induced membrane repolarization or hyperpolarization due to activation of Ca^{2+}-activated K^+ channels in PASMC.[68]

Chronic hypoxic exposure of mice inhibits acute alveolar hypoxia-induced pulmonary vasoconstriction

Early studies showed that chronic exposure of mice (and rats) to hypoxia enhances pulmonary vasoconstrictive reactivity in response to various agonists,[12] while humans living in high altitude have blunted response to acute hypoxia.[69] In rats, it has been reported that acute HPV was significantly inhibited in chronically hypoxic rats.[32,70–72] In this study, we examined whether chronic hypoxia-mediated structural changes in the pulmonary vasculature affects acute HPV. Mice were first exposed to hypoxia for four weeks, which led to significant increases in (*a*) right ventricular systolic pressure (Fig. 7a), a surrogate measurement of pulmonary arterial systolic pressure, (*b*) right ventricular contractility (i.e. RV-± dP/dt_{max}) (Fig. 7b), and (*c*) Fulton Index, the ratio of the weight of LV to the weight of LV and septum (S) (RV/(LV + S)) (Fig. 7c) in comparison to normoxic controls. The heart rate in normoxic control mice (507 ± 24 beats/min, $n = 11$) and chronically hypoxic mice (488 ± 28 beats/min, $n = 8$) was not changed significantly ($p = 0.611$). Following chronic hypoxic exposure, the lung

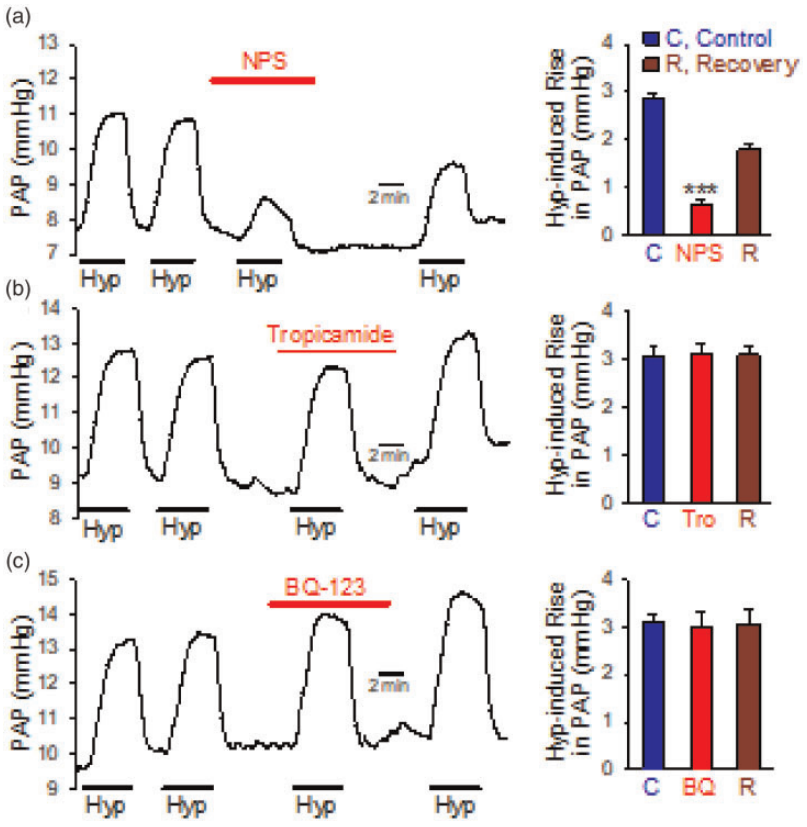

Fig. 4. Blockade of calcium sensing receptor (CaSR) significantly inhibits hypoxia-induced increase in pulmonary arterial pressure (PAP) in isolated perfused/ventilated mouse lungs. (a–c) Representative records (left panels) showing changes of PAP induced by ventilation of hypoxic gas (1% O_2 in N_2 for 4 min) before, during, and after perfusion of NPS 2143 (NPS, 30 μM, an allosteric CaSR antagonist, a), tropicamide (TRO, 10 μM, a muscarinic receptor antagonist, b), or BQ-123 (BQ, 10 μM, an endothelin receptor A antagonist, c). Summarized data (means ± SE, right panels, $n = 5$ mouse lungs) showing the hypoxia-induced increases in PAP before (Control, c), during, and after (Recovery, R) perfusion with PSS containing NPS, Tro, or BQ, respectively. ***$p < 0.001$ vs Control (C, blue) bars and Recovery (R, dark red) bars.

vasculature underwent significant changes revealed by angiography (Fig. 7d and e). The total length of vascular branches, the number of branches, and the number of junctions between vascular branches were all significantly decreased in the lungs from chronically hypoxic mice compared to normoxic controls (Fig. 7d and e). These data show that chronic hypoxia resulted in significant pulmonary vascular remodeling.

Then, we examined and compared the basal PAP, determined by measuring the basal pulmonary vascular pressure under the constant flow rate of perfusion, and the amplitude of acute (5 min) alveolar hypoxia-induced increase in PAP in isolated perfused/ventilated lungs from normoxic control mice and chronically hypoxic mice. As shown in Fig. 7f and g, when the perfusion rate was maintained at the same level, the basal PAP in the isolated perfused/ventilated lungs from chronically hypoxic lungs was significantly higher than that in the isolated lungs from normoxic control mice (Fig. 7f). The increased basal PAP in the isolated perfused/ventilated lungs from chronically hypoxic mice was due apparently to the chronic hypoxia-induced structural changes in the pulmonary vasculature (Fig. 7d), including concentric pulmonary arterial wall thickening due to medial hypertrophy. In the isolated perfused/ventilated lungs from chronically hypoxic mice, acute alveolar hypoxia (for 5 min) was still able to induce a decent increase in PAP (Fig. 7f). The amplitude of acute alveolar hypoxia-induced PAP increases in isolated lungs of chronically hypoxic mice, however, was significantly diminished in comparison to the lungs from normoxic control mice (Fig. 7f and g). These data indicate that chronic hypoxia-mediated pulmonary vascular remodeling or structural changes diminished the pulmonary vascular reactivity in response to acute alveolar hypoxia. The chronic hypoxia-mediated pulmonary vascular remodeling may enhance the pulmonary vascular reactivity to other agonists.[12]

Discussion

In this study, we used the isolated perfused/ventilated mouse lung model, previously optimized by our laboratory,[5] to revisit the Ca^{2+} signaling mechanisms involved in acute HPV. Specifically, we focused on the potential roles of voltage-dependent/independent Ca^{2+} and Cl^- channels as well as GPCRs and Notch receptors. The ex vivo experiments indicate that HPV is primarily dependent of Ca^{2+} influx

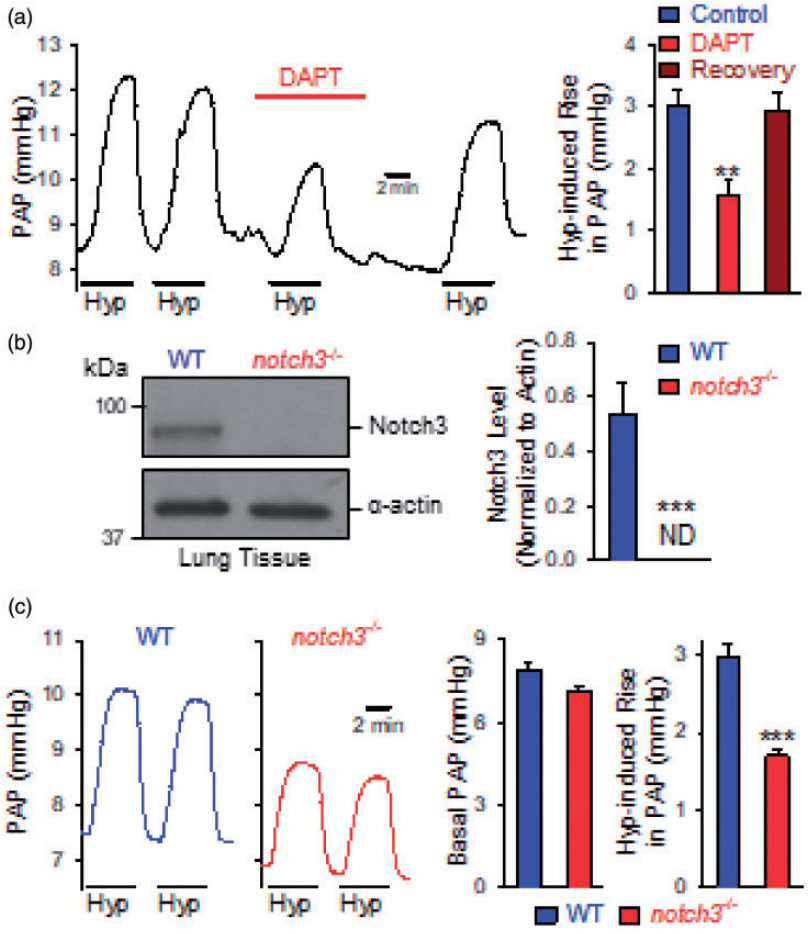

Fig. 5. Inhibition of Notch signaling attenuates hypoxia-induced increase in pulmonary arterial pressure (PAP) in isolated perfused/ventilated mouse lungs. (a) Representative records (left panel) showing changes of PAP induced by ventilation of hypoxic gas (1% O_2 in N_2 for 4 min) before, during, and after perfusion of DAPT (30 μM, a γ-secretase inhibitor). Summarized data (means ± SE, right panel, $n = 5$ mouse lungs) showing the hypoxia-induced increases in PAP before (Cont), during (DAPT), and after (Rec) perfusion with PSS containing DAPT. (b) Representative Western blot images (left panel) and summarized data (means ± SE, right panel, $n = 3$ independent experiments from five mice) showing Notch3 expression levels in lung tissues isolated from WT and *notch3*$^{-/-}$ mice. ***$p < 0.001$ vs. WT. (c) Representative records (left panels) of PAP before, during, and after ventilation of hypoxic gas (1% O_2 in N_2 for 4 min) in WT and Notch3 knock-out (*notch3*$^{-/-}$) mice. Summarized data (means ± SE, $n = 5$ mouse lungs, right panel) showing acute hypoxia-induced increase in PAP in WT and *notch3*$^{-/-}$ mice. ***$p < 0.001$ vs. WT (c). ND: not detectable.

through various voltage-dependent and -independent Ca^{2+} channels in PASMC; the process is regulated or modulated by Notch and CaSR signaling cascades. Removal of extracellular Ca^{2+} abolished HPV, while blockade of voltage-dependent Ca^{2+} entry through L-type VDCC and receptor-operated Ca^{2+} entry through TRP channels significantly and reversibly inhibited HPV. These data also indicate that the mechanism of HPV or acute hypoxia-induced Ca^{2+} influx is not due to a single pathway[3]; multiple ion channels and signaling cascades are involved to ensure HPV. Since there is no appropriate morphometric technique to evaluate the whole pulmonary vascular tree quantitatively, the isolated perfused/ventilated lung is an excellent ex vivo model to study the mechanisms involved in HPV. The use of knockout (KO) mice provides more convincing data on the role of different proteins and genes played in the initiation and regulation of HPV.

$[Ca^{2+}]_{cyt}$ in PASMC can be increased by Ca^{2+} influx through various cation channels in the plasma membrane and Ca^{2+} release or mobilization from individual intracellular stores.[73] In PASMC, there are at least three classes of Ca^{2+}-permeable channels responsible for Ca^{2+} influx: (*a*) VDCC which are opened by membrane depolarization, (*b*) ROC which are opened by DAG upon receptor activation, and (*c*) SOC which are opened by a reduction of $[Ca^{2+}]$ level in the SR due to active or passive depletion of stored Ca^{2+}.[12,74,75] Activity of Na^+ pump (or Na^+/K^+ ATPase) and K^+ channel play a vital role in maintaining and regulating the resting membrane potential (E_m) in PASMC. Acute hypoxia has been demonstrated to inhibit K^+ channels,[76] which subsequently causes membrane depolarization and opening of VDCC thereby increasing $[Ca^{2+}]_{cyt}$ in PASMC.[7,77–80] The acute hypoxia-mediated increase in $[Ca^{2+}]_{cyt}$ by membrane depolarization is believed to be, at

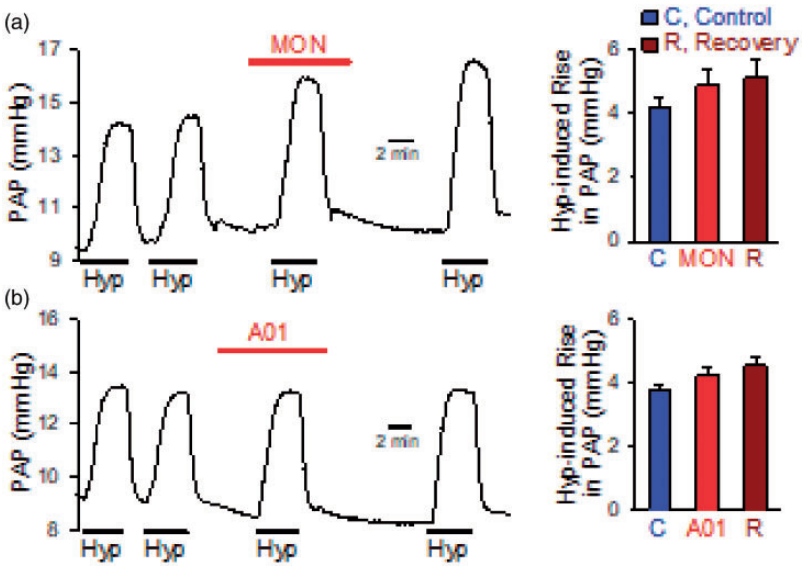

Fig. 6. Blockade of Ca^{2+}-activated Cl^- (Cl_{Ca}) channels fails to inhibit hypoxia-induced rise in pulmonary arterial pressure (PAP) in isolated perfused/ventilated mouse lungs. (a and b) Representative records (left panels) showing changes of PAP induced by ventilation of hypoxic gas (1% O_2 in N_2 for 4 min) before, during, and after perfusion of MONNA (MON, 10 μM, a TMEM16A/anoctamin-1 blocker, a), CaCCinh-A01 (A01, 10 μM, a Cl_{Ca} channel blocker, b). Summarized data (means ± SE, right panels, $n = 5$ mouse lungs) showing the hypoxia-induced increases in PAP before (Control), during, and after (Recovery) perfusion with PSS containing MON (a) or A01 (b).

least, mediated by Ca^{2+} influx through L-type VDCC formed by the pore-forming subunits $Ca_V1.1$ (α_{1S}), $Ca_V1.2$ (α_{1C}), $Ca_V1.3$ (α_{1D}), and/or $Ca_V1.4$ (α_{1F}).[66] The results from this study show that only blockade of L-type of VDCC inhibits HPV, whereas the blockers for T-, N-, P-, and Q-type of VDCC seem to have little effect on HPV. Although Nif is a dihydropyridine Ca^{2+} channel blocker that selectively blocks L-type VDCC,[81–83] Nif and other dihydropyridine VDCC blockers have been shown to inhibit the adenosine A_{2B} receptor, a GPCR in colonic tissues and cells.[84] The inhibitory effect of Nif on adenosine A_{2B} receptors has been implicated having therapeutic potential for diarrhea and related diseases.[84] In addition, it has been shown that T-type of VDCC is involved in hypoxia-induced PH in rats[85]; but more experiments are needed to define the role of different types of VDCC in the initiation and regulation of HPV.

Acute hypoxia-mediated increase in $[Ca^{2+}]_{cyt}$ may also result from Ca^{2+} influx through ROC formed by the TRP channels. Indeed, blockade of non-selective cation channels formed by TRP channels significantly inhibited HPV, while isolated perfused/ventilated lungs from *trpc6*$^{-/-}$ mice exhibit significantly reduced amplitude of HPV in comparison to WT littermates (see Fig. 3g).[86] TRPC6 channel is an important ROC in smooth muscle cells[87–89] and is functionally coupled to CaSR, a GPCR, to mediate CaSR-associated Ca^{2+} influx in PASMC.[20,90] The data from this study imply that CaSR-associated Ca^{2+} influx through ROC formed by TRP channels (e.g. TRPC6) is also an important pathway for hypoxia-induced increase of $[Ca^{2+}]_{cyt}$ in PASMC and HPV. One of the concerns with regard to the pharmacological experiments using different TRPC inhibitors is lack of potent and selective inhibitor for TRPC6. SKF-96365 is a non-selective blocker of TRPC6 and other TRPC channels (e.g. TRPC3 and TRPC7).[91] Furthermore, it has been reported that SKF-96365 also blocks T-type of VDCC; the SKF-96365 seems to induce more potent blockade effect on VDCC than on TRPC3. SKF-96365 has been shown to block other subtypes of VDCC (including L-type, N-type, and P/Q-type).[92] Another TRPC6 antagonist, SAR-7334, can also bind to TRPC3 and TRPC7.[47] Recently, another potent, selective and orally available TRPC6 blocker, BI749327, has been shown to have promising therapeutic effects on renal and cardiac fibrosis.[93] Apart from TRPC channels, TRPV channels (e.g. TRPV4) have also been implicated in HPV.[94] Our data in this study show that blockade of TRPV1 channels with CPZ reversibly inhibit acute HPV. However, CPZ may also non-specifically bind to nicotine ACh receptors and TRPM8 channels.[95] Furthermore, TRPV1 and TRPV4 also contribute to capsaicin- and serotonin-induced pulmonary vasoconstriction, respectively,[48] while TRPV4 is also implicated in chronic hypoxia-induced PH.[94]

Our ex vivo data from this study indicate that CaSR receptors are involved in or required for HPV. Activation of CaSR increases IP_3 and DAG. IP_3 activates IP_3R in the SR and induces Ca^{2+} mobilization, while DAG activates ROC in the plasma membrane and induces receptor operated calcium entry (ROCE). Both IP_3-mediated Ca^{2+} mobilization and DAG-mediated Ca^{2+} influx contribute to increasing $[Ca^{2+}]_{cyt}$ in PASMC that is required for causing pulmonary vasoconstriction.[96–98] Therefore, ROCE induced by DAG-mediated activation of ROC (formed by TRPC6 and TRPV1, for example) and SOCE induced by the IP_3R–

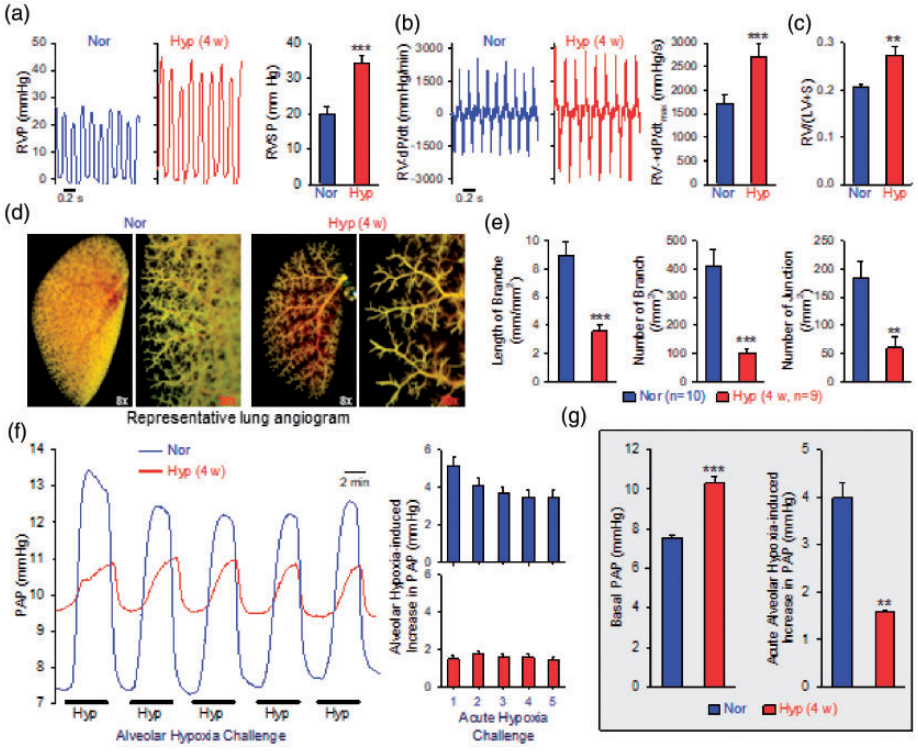

Fig. 7. Acute hypoxia-induced pulmonary vasoconstriction is inhibited in isolated perfused/ventilated from mice with chronic hypoxia-mediated pulmonary hypertension. (a): Representative records showing right ventricular pressure (RVP, left panels) and summarized data (means ± SE, $n = 5–8$, right panel) showing right ventricular systolic pressure (RVSP), a surrogate measurement of pulmonary arterial systolic pressure, in normoxic control mice (Nor), and chronically hypoxic mice (for four weeks, Hyp-4w). ***$p < 0.001$ vs. Nor. (b): Representative record showing right ventricle (RV) ± dP/dt (RV- ± dP/dt, left panels) and summarized data (means ± SE, $n = 5–8$, right panel) showing the maximal RV ± dP/dt (RV ± dP/dt_{max}) values in Nor and Hyp-4w mice. ***$p < 0.001$ vs. Nor. (c): Fulton index, the ratio of the weight of right ventricle (RV) to the weight of left ventricle (LV), and septum (S) (RV/(LV + S)) of the heart isolated from in Nor and Hyp-4w mice. (d): Representative angiographic images (8 × or 30 × in magnification) showing the pulmonary vascular structure in a Nor control mouse (left) and a Hyp-4w mouse (right). The 30 × image in right shows a peripheral region of the whole lung (8 × image). (e): Summarized data (means ± SE, $n = 9–10$) showing the total length of pulmonary vascular branches (left), the number of branches (middle), and the number of junctions of the vascular branches (right) in Nor control mice (blue) and chronically hypoxic (Hyp-4w) mice (red). **$p < 0.01$, ***$p < 0.001$ vs. normoxic control. (f): Representative record showing changes of pulmonary arterial pressure (PAP) before, during, and after acute ventilation of hypoxic gas mixture (Hyp, 1% O_2 in N_2, for 4 min in each challenge) in isolated perfused/ventilated lungs from a normoxic (Nor) control mouse (blue) and a chronically hypoxic (Hyp-4w) mouse (red). The averaged data (means ± SE, $n = 8–10$ mice) showing the increase in PAP induced by a series of consecutive hypoxia challenges. (g): Summarized data (means ± SE, $n = 8–10$) showing the basal PAP (left) and acute alveolar hypoxia-induced increases in PAP (right) in isolated perfused/ventilated lungs from Nor mice (blue) and Hyp-4w mice (red). **$p < 0.01$, ***$p < 0.001$ vs. Nor.

STIM interaction and IP_3-induced active store depletion (upon activation of membrane receptors like CaSR in the plasma membrane) are all involved in triggering HPV. Interestingly, it has been reported that in rabbit portal vein smooth muscle cells, TRPC6/7 channels can be activated independent of DAG by eliminating the inhibitory response of phosphatidylinositol 4,5-bis phosphate.[99] The results from this study also indicate a potential role of Notch activation in HPV. Inhibition of γ-secretase with DAPT significantly attenuates HPV, while *notch3*$^{-/-}$ mice exhibit significantly reduced amplitude of HPV (Fig. 5). These data suggest that NICD may participate in regulating HPV. These data confirmed our previously published results and we further showed that hypoxia activated Notch signaling, which enhances SOCE via direct interaction with TRPC6 leading to HPV and development of chronic hypoxia-induced PH. Thus, Notch signaling is involved in regulation of cytosolic Ca^{2+}.[43] It is, however, unknown whether and how NICD is involved in enhancing CaSR-mediated ROCE/SOCE and/or IP3R/STIM interaction in PASMC.[100] Recently, it was shown that DAPT, a γ-secretase inhibitor that inhibits Notch signaling, also attenuated pulmonary fibrosis in mice through inhibition of pericyte proliferation and transition.[101]

In vascular smooth muscle cells, intracellular [Cl^-] is very high so the equilibrium potential for Cl^- is less negative than the resting membrane potential. Activation of Cl^- channels under resting conditions would thus cause Cl^- efflux and membrane depolarization.[102] Ca^{2+}-activated Cl^- (Cl_{Ca}) channels, formed by TMEM16A, are expressed in arterial smooth muscle cells and exert an important role in the regulation of smooth muscle excitation–contraction coupling

and vascular tone.[103–105] It has been demonstrated that Cl_{Ca} channels or TMEM16A are upregulated in PASMC of chronically hypoxic rats and monocrotaline-treated rats,[106,107] while increased activity of Cl_{Ca} channels (formed by TMEM16A) is an important contributor to the changes in electromechanical coupling of PA and membrane depolarization in PASMC from animals with experimental PH.[107] In the current study, however, intrapulmonary superfusion of the Ca^{2+}-activated Cl^- channel blockers, MONNA and A01, had little effect on HPV. Though, MONNA was claimed to be a selective blocker of TMEM16 Ca^{2+}-activated Cl^- channels, its selectivity has been challenged by a study which showed that MONNA induced dose-dependent relaxation in rat mesenteric arteries in the absence of Cl^- gradient.[108] Recently, it was reported that chronic administration of benzbromarone attenuated pulmonary vascular remodeling in two different experimental models of PH through inhibition of TMEM16A.[109] Inhibition of cystic fibrosis transmembrane conductance regulator (CFTR), a Cl^- channel that is also permeable to HCO_3^-,[110,111] significantly attenuated HPV.[112] In PASMC, hypoxia causes CFTR to interact with TRPC6. Inhibition of CFTR attenuates hypoxia-induced TRPC6 translocation to caveolae and sphingosine-1-phosphate-mediated Ca^{2+} mobilization in PASMC. These data indicate that sphingolipid-mediated interaction of CFTR, a $Cl^-/HCO3^-$ channel, and TRPC6, a non-selective cation channel, in PASMC plays an important role in HPV.[112]

It is clear from our data that Ca^{2+} influx through various Ca^{2+}-permeable cation channels is involved in the initiation of HPV; however, Ca^{2+}-independent activation of Rho kinase and enhancement of Ca^{2+} sensitivity of contractile proteins have also been implicated in the development of HPV.[113] Hypoxia seems to be able to activate Rho kinase in both PASMCs and endothelial cells.[38,113,114] Rho kinase appears to play an important role in mediating both the acute and chronic effects of hypoxia on pulmonary circulation.[115]

Alveolar hypoxia induces pulmonary vasoconstriction to match the perfusion with ventilation ensuring maximal oxygenation of the venous blood in PA. Persistent hypoxia, however, causes sustained pulmonary vasoconstriction and excessive pulmonary vascular remodeling and subsequently PH.[116,117] It has been demonstrated that chronic alveolar hypoxia downregulates Kv channels and upregulates TRP channels in PASMC causing pulmonary vasoconstriction and vascular remodeling.[118,119] In 1978, McMurtry and colleagues reported that lungs from chronically hypoxic rats have decreased acute hypoxia-mediated pulmonary vasoconstriction.[72] In mice, we observed the same results that chronic exposure of mice to hypoxia for four weeks resulted in PH characterized by significant pulmonary vascular remodeling; however, the acute HPV was significantly inhibited in isolated perfused/ventilated lungs from chronically hypoxic mice (Fig. 7). These data imply that acute hypoxia induces pulmonary vasoconstriction by mechanisms that may be shared by chronic hypoxia to induce pulmonary vasoconstriction and vascular remodeling. The proposed mechanisms include impaired lung vascular endothelial function,[70] mitochondrial dysfunction[120–122] and metabolic shift,[123,124] functional and transcriptional changes of ion channels and membrane receptors,[3] and Ca^{2+}-sensitive intracellular signaling proteins and transcription factors.[125]

Here, we used an ex vivo mouse model, isolated perfused/ventilated lung preparation, for a series of comprehensive pharmacological experiments to define the Ca^{2+} signaling mechanisms involved in acute hypoxia-induced pulmonary vasoconstriction. The isolated perfused/ventilated lung model we used in this study has both strengths and drawbacks, but we believe the benefits outweigh the drawbacks. To investigate the precise mechanisms of HPV, investigators have used intact animals, isolated lungs, isolated pulmonary arteries, and freshly-dissociated and primary cultured PASMC and endothelial cells.[41,79,126] Studies in vessels or arterial rings provide important information about, for example, two phases of HPV and the involvement of contractile proteins and the involvement of contractile proteins and Ca^{2+}-sensitive and -insensitive signaling proteins. However, results obtained from freshly-dissociated or primary cultured cells are very different from the vessels or the whole vasculature in isolated lungs or the intact animals. One of the advantages of using the isolated perfused lung to study HPV is that it minimizes the impact of systemic organs[127] while maintaining the intact lungs and allowing a more physiological setting for transport of solutes across capillary membrane and exchange of O_2 and CO_2 across the blood–air barrier.[128] Although acute hypoxia causes vasoconstriction in isolated vessels or rings, the kinetics of HPV response in vessels or rings is different from HPV in humans and intact animals. In isolated perfused/ventilated lungs, the kinetics of HPV is similar to that in intact animals and humans. Overall, the advantage of using the isolated perfused/ventilated lung to study HPV is that (*i*) it reflects the functional changes of the whole lung vasculature, (*ii*) it introduces alveolar hypoxia via ventilation to the vasculature (instead of using hypoxemic solution to perfuse into the vessels), (*iii*) it allows us to superfuse inhibitors via perfusion pump into PA or the pulmonary vasculature to examine their effect; (*iv*) it shows very similar time-course shown in intact animals and healthy subjects; (*v*) it minimizes the impact of other organs and nervous systems on HPV while maintaining the intact lung in a relatively physiological setting (e.g. the preparation is consistently ventilated through the airway and alveoli, and perfused through the pulmonary arteries, capillaries, and vens); and (*vi*) it allows us to examine whether genetic deletion (e.g. KO mice) or overexpression (e.g. transgenic mice) of specific genes affects HPV.

The data from our study indicate that extracellular Ca^{2+}, or Ca^{2+} influx through various Ca^{2+}-permeable channels in the plasma membrane, is required for HPV. Removal of extracellular Ca^{2+} abolished HPV, while blockade of L-type VDCC (with Nif), non-selective cation channels

(with SKF) and TRP channels (with SAR and CPZ) significantly and reversibly inhibited HPV. Furthermore, blockers of CaSR and Notch receptors also attenuated HPV. These results led us to conclude that Ca^{2+} influx through L-type voltage-gated Ca^{2+} channels and TRPC6-formed ROC plays an important role in the initiation of pulmonary vasoconstriction during alveolar hypoxia; however, contribution of Ca^{2+} channels in the plasma membrane and cation channels in the intracellular organelles to the regulation of HPV cannot be ruled out. From our study, we have confirmed our and other investigators' data on the critical role of Ca^{2+} signaling in HPV. We believe that present pharmacological study utilizing various inhibitors of ion channels and membrane receptors in isolated perfused/ventilated mouse lung model provides data giving us a comprehensive overview on the involvement of ion channels and membrane receptors in HPV. Furthermore, the results of our study could serve as a template for selecting inhibitors for the future research.

In this study, we also included mouse angiography images showing left and right lungs from normoxic control and chronically hypoxic C57Bl/6 J mice with detailed quantification (i.e. the total length of lung vascular branches, the number of vascular branches, and the number of junctions among branches). The mouse lung angiography data can be used as a template to further study chronic hypoxia-mediated pulmonary vascular remodeling in WT mice and various KO and transgenic mice. The mouse lung angiography technique is a simple and economic method in comparison to the expensive micro-CT imaging approach.[129]

In summary, the data from this study indicate that Ca^{2+} influx through voltage-gated, receptor-operated, and SOC in the plasma membrane of PASMC plays an important role in the initiation of HPV, while the extracellular Ca^{2+}-mediated activation of CaSR and the cell–cell interaction via Notch ligands and receptors contribute to the regulation of HPV.

Author contributions

Jason X.-J. Yuan initiated the project and designed the study. Pritesh P. Jain wrote the initial draft of the manuscript, performed most of the experiments, and conducted data analysis. Susumu Hosokawa, Aleksandra Babicheva, Mingmei Xiong, Tengteng Zhao, Marisela Rodriguez, Shamin Rahimi, Francesca Balistrieri, Kiana Pourhashemi, and Ning Lai assisted in performing the experiments and in acquiring/analyzing data. Daniela Valdez-Jasso, Patricia A. Thistlethwaite, Atul Malhotra, John Y.-J. Shyy, and Ayako Makino participated in the discussion on experimental design and critically reviewed the manuscript.

Conflict of interest

The author(s) declare that there is no conflict of interest.

Funding

This work is supported in part by the grants from the National Heart, Lung and Blood Institute of the National Institutes of Health (R35 HL135807 and R01 HL146764).

ORCID iD

Ayako Makino https://orcid.org/0000-0003-1259-8604

References

1. Weir EK and Archer SL. The mechanism of acute hypoxic pulmonary vasoconstriction: the tale of two channels. *FASEB J* 1995; 9: 183–189.
2. Euler USv and Liljestrand G. Observations on the pulmonary arterial blood pressure in the cat. *Acta Physiol Scand* 1946; 12: 301–320.
3. Sylvester JT, Shimoda LA, Aaronson PI, et al. Hypoxic pulmonary vasoconstriction. *Physiol Rev* 2012; 92: 367–520.
4. Sommer N, Strielkov I, Pak O, et al. Oxygen sensing and signal transduction in hypoxic pulmonary vasoconstriction. *Eur Respir J* 2016; 47: 288–303.
5. Yoo HY, Zeifman A, Ko EA, et al. Optimization of isolated perfused/ventilated mouse lung to study hypoxic pulmonary vasoconstriction. *Pulm Circ* 2013; 3: 396–405.
6. McMurtry IF, Davidson AB, Reeves JT, et al. Inhibition of hypoxic pulmonary vasoconstriction by calcium antagonists in isolated rat lungs. *Circ Res* 1976; 38: 99–104.
7. Post JM, Hume JR, Archer SL, et al. Direct role for potassium channel inhibition in hypoxic pulmonary vasoconstriction. *Am J Physiol* 1992; 262: C882–C890.
8. Brayden JE and Nelson MT. Regulation of arterial tone by activation of calcium-dependent potassium channels. *Science* 1992; 256: 532–535.
9. Tucker A, McMurtry IF, Grover RF, et al. Attenuation of hypoxic pulmonary vasoconstriction by verapamil in intact dogs. *Proc Soc Exp Biol Med* 1976; 151: 611–614.
10. Joshi S, Balan P and Gurney AM. Pulmonary vasoconstrictor action of KCNQ potassium channel blockers. *Respir Res* 2006; 7: 31.
11. Yamamura A, Yamamura H, Guo Q, et al. Dihydropyridine Ca^{2+} channel blockers increase cytosolic [Ca^{2+}] by activating Ca^{2+}-sensing receptors in pulmonary arterial smooth muscle cells. *Circ Res* 2013; 112: 640–650.
12. Wan J, Yamamura A, Zimnicka AM, et al. Chronic hypoxia selectively enhances L- and T-type voltage-dependent Ca^{2+} channel activity in pulmonary artery by upregulating Cav1.2 and Cav3.2. *Am J Physiol Lung Cell Mol Physiol* 2013; 305: L154–L164.
13. Yamamura A, Yamamura H, Guo Q, et al. Dihydropyridine Ca^{2+} channel blockers increase cytosolic [Ca^{2+}] by activating Ca^{2+}-sensing receptors in pulmonary arterial smooth muscle cells. *Circ Res* 2013; 112: 640–650.
14. Beasley D, Cohen RA and Levinsky NG. Interleukin 1 inhibits contraction of vascular smooth muscle. *J Clin Invest* 1989; 83: 331–335.
15. Tsien RW and Tsien RY. Calcium channels, stores, and oscillations. *Annu Rev Cell Biol* 1990; 6: 715–760.
16. Franco-Obregon A and Lopez-Barneo J. Differential oxygen sensitivity of calcium channels in rabbit smooth muscle cells of conduit and resistance pulmonary arteries. *J Physiol* 1996; 491: 511–518.
17. Zamponi GW, Striessnig J, Koschak A, et al. The physiology, pathology, and pharmacology of voltage-gated calcium channels and their future therapeutic potential. *Pharmacol Rev* 2015; 67: 821–870.

18. Kuga T, Kobayashi S, Hirakawa Y, et al. Cell cycle-dependent expression of L- and T-type Ca^{2+} currents in rat aortic smooth muscle cells in primary culture. *Circ Res* 1996; 79: 14–19.
19. Zhang Y, Lu W, Yang K, et al. Bone morphogenetic protein 2 decreases TRPC expression, store-operated Ca^{2+} entry, and basal $[Ca^{2+}]_i$ in rat distal pulmonary arterial smooth muscle cells. *Am J Physiol Cell Physiol* 2013; 304: C833–C843.
20. Tang H, Yamamura A, Yamamura H, et al. Pathogenic role of calcium-sensing receptors in the development and progression of pulmonary hypertension. *Am J Physiol Lung Cell Mol Physiol* 2016; 310: L846–L859.
21. Song S, Carr SG, McDermott KM, et al. STIM2 (stromal interaction molecule 2)-mediated increase in resting cytosolic free Ca^{2+} concentration stimulates PASMC proliferation in pulmonary arterial hypertension. *Hypertension* 2018; 71: 518–529.
22. Kuhr FK, Smith KA, Song MY, et al. New mechanisms of pulmonary arterial hypertension: role of Ca^{2+} signaling. *Am J Physiol Heart Circ Physiol* 2012; 302: H1546–H1562.
23. Mandegar M, Remillard CV and Yuan JX. Ion channels in pulmonary arterial hypertension. *Prog Cardiovasc Dis* 2002; 45: 81–114.
24. Wright DB, Tripathi S, Sikarwar A, et al. Regulation of GPCR-mediated smooth muscle contraction: implications for asthma and pulmonary hypertension. *Pulm Pharmacol Ther* 2013; 26: 121–131.
25. Faber JE, Szymeczek CL, Cotecchia S, et al. α1-adrenoceptor-dependent vascular hypertrophy and remodeling in murine hypoxic pulmonary hypertension. *Am J Physiol Heart Circ Physiol* 2007; 292: H2316–H2323.
26. Peyter A-C, Muehlethaler V, Liaudet L, et al. Muscarinic receptor M1 and phosphodiesterase 1 are key determinants in pulmonary vascular dysfunction following perinatal hypoxia in mice. *Am J Physiol Lung Cell Mol Physiol* 2008; 295: L201–L213.
27. Iglarz M, Steiner P, Wanner D, et al. Vascular effects of endothelin receptor antagonists depends on their selectivity for ET_A versus ET_B receptors and on the functionality of endothelial ET_B receptors. *J Cardiovasc Pharmacol* 2015; 66: 332–337.
28. Sato K, Morio Y, Morris KG, et al. Mechanism of hypoxic pulmonary vasoconstriction involves ET_A receptor-mediated inhibition of K_{ATP} channel. *Am J Physiol Lung Cell Mol Physiol* 2000; 278: L434–L442.
29. Zhang WM, Yip KP, Lin MJ, et al. ET-1 activates Ca^{2+} sparks in PASMC: local Ca^{2+} signaling between inositol trisphosphate and ryanodine receptors. *Am J Physiol Lung Cell Mol Physiol* 2003; 285: L680–L690.
30. Cybulsky AV, Carbonetto S, Cyr MD, et al. Extracellular matrix-stimulated phospholipase activation is mediated by β1-integrin. *The Am J Physiol* 1993; 264: C323–C332.
31. Wang J, Weigand L, Foxson J, et al. Ca^{2+} signaling in hypoxic pulmonary vasoconstriction: effects of myosin light chain and Rho kinase antagonists. *Am J Physiol Lung Cell Mol Physiol* 2007; 293: L674–L685.
32. Fagan KA, Oka M, Bauer NR, et al. Attenuation of acute hypoxic pulmonary vasoconstriction and hypoxic pulmonary hypertension in mice by inhibition of Rho-kinase. *Am J Physiol Lung Cell Mol Physiol* 2004; 287: L656–L664.
33. Keseru B, Barbosa-Sicard E, Schermuly RT, et al. Hypoxia-induced pulmonary hypertension: comparison of soluble epoxide hydrolase deletion vs inhibition. *Cardiovasc Res* 2010; 85: 232–240.
34. Fuchs B, Rupp M, Ghofrani HA, et al. Diacylglycerol regulates acute hypoxic pulmonary vasoconstriction via TRPC6. *Respir Res* 2011; 12: 20.
35. Karamsetty MR, Klinger JR and Hill NS. Evidence for the role of p38 MAP kinase in hypoxia-induced pulmonary vasoconstriction. *Am J Physiol Lung Cell Mol Physiol* 2002; 283: L859–L866.
36. Aaronson PI, Robertson TP, Knock GA, et al. Hypoxic pulmonary vasoconstriction: mechanisms and controversies. *J Physiol* 2006; 570: 53–58.
37. Rathore R, Zheng YM, Li XQ, et al. Mitochondrial ROS-PKCε signaling axis is uniquely involved in hypoxic increase in $[Ca^{2+}]_i$ in pulmonary artery smooth muscle cells. *Biochem Biophys Res Commun* 2006; 351: 784–790.
38. Wang Z, Jin N, Ganguli S, et al. Rho-kinase activation is involved in hypoxia-induced pulmonary vasoconstriction. *Am J Respir Cell Mol Biol* 2001; 25: 628–635.
39. Waypa GB and Schumacker PT. O_2 sensing in hypoxic pulmonary vasoconstriction: the mitochondrial door re-opens. *Respir Physiol Neurobiol* 2002; 132: 81–91.
40. Zheng YM, Wang QS, Rathore R, et al. Type-3 ryanodine receptors mediate hypoxia-, but not neurotransmitter-induced calcium release and contraction in pulmonary artery smooth muscle cells. *J Gen Physiol* 2005; 125: 427–440.
41. Moudgil R, Michelakis ED and Archer SL. Hypoxic pulmonary vasoconstriction. *J Appl Physiol* 2005; 98: 390–403.
42. Li X, Zhang X, Leathers R, et al. Notch3 signaling promotes the development of pulmonary arterial hypertension. *Nat Med* 2009; 15: 1289–1297.
43. Smith KA, Voiriot G, Tang H, et al. Notch activation of $Ca^{(2+)}$ signaling in the development of hypoxic pulmonary vasoconstriction and pulmonary hypertension. *Am J Respir Cell Mol Biol* 2015; 53: 355–367.
44. Chevalier M, Gilbert G, Roux E, et al. T-type calcium channels are involved in hypoxic pulmonary hypertension. *Cardiovasc Res* 2014; 103: 597–606.
45. Fu XW, Nurse CA, Wong V, et al. Hypoxia-induced secretion of serotonin from intact pulmonary neuroepithelial bodies in neonatal rabbit. *J Physiol* 2002; 539: 503–510.
46. Papp R, Nagaraj C, Zabini D, et al. Targeting TMEM16A to reverse vasoconstriction and remodelling in idiopathic pulmonary arterial hypertension. *Eur Respir J* 2019; 53.
47. Maier T, Follmann M, Hessler G, et al. Discovery and pharmacological characterization of a novel potent inhibitor of diacylglycerol-sensitive TRPC cation channels. *Br J Pharmacol* 2015; 172: 3650–3660.
48. Song S, Ayon RJ, Yamamura A, et al. Capsaicin-induced Ca^{2+} signaling is enhanced via upregulated TRPV1 channels in pulmonary artery smooth muscle cells from patients with idiopathic PAH. *Am J Physiol Lung Cell Mol Physiol* 2017; 312: L309–L325.
49. Dai X-Q, Ramji A, Liu Y, et al. Inhibition of TRPP3 Channel by Amiloride and Analogs. *Mol Pharmacol* 2007; 72: 1576–1585.
50. Schenkel LB, Olivieri PR, Boezio AA, et al. Optimization of a novel quinazolinone-based series of transient receptor potential A1 (TRPA1) antagonists demonstrating potent in vivo activity. *J Med Chem* 2016; 59: 2794–2809.

51. Earley S, Waldron BJ and Brayden JE. Critical role for transient receptor potential channel TRPM4 in myogenic constriction of cerebral arteries. *Circ Res* 2004; 95: 922–929.
52. Nagata K, Zheng L, Madathany T, et al. The varitint-waddler (Va) deafness mutation in TRPML3 generates constitutive, inward rectifying currents and causes cell degeneration. *Proc Natl Acad Sci U S A* 2008; 105: 353–358.
53. Yamamura A, Guo Q, Yamamura H, et al. Enhanced Ca^{2+}-sensing receptor function in idiopathic pulmonary arterial hypertension. *Circ Res* 2012; 111: 469–481.
54. Hernandez M, Simonsen U, Prieto D, et al. Different muscarinic receptor subtypes mediating the phasic activity and basal tone of pig isolated intravesical ureter. *Br J Pharmacol* 1993; 110: 1413–1420.
55. Inoue R, Jensen LJ, Jian Z, et al. Synergistic activation of vascular TRPC6 channel by receptor and mechanical stimulation via phospholipase C/diacylglycerol and phospholipase A2/Ω-hydroxylase/20-HETE pathways. *Circ Res* 2009; 104: 1399–1409.
56. Liu D, Yang D, He H, et al. Increased transient receptor potential canonical type 3 channels in vasculature from hypertensive rats. *Hypertension* 2009; 53: 70–76.
57. Baba Y and Kurosaki T. Physiological function and molecular basis of STIM1-mediated calcium entry in immune cells. *Immunol Rev* 2009; 231: 174–188.
58. Earley S and Brayden JE. Transient receptor potential channels in the vasculature. *Physiol Rev* 2015; 95: 645–690.
59. Weigand L, Foxson J, Wang J, et al. Inhibition of hypoxic pulmonary vasoconstriction by antagonists of store-operated Ca^{2+} and nonselective cation channels. *Am J Physiol Lung Cell Mol Physiol* 2005; 289: L5–L13.
60. Galie N, Manes A and Branzi A. The endothelin system in pulmonary arterial hypertension. *Cardiovasc Res* 2004; 61: 227–237.
61. Norel X, Walch L, Costantino M, et al. M1 and M3 muscarinic receptors in human pulmonary arteries. *Br J Pharmacol* 1996; 119: 149–157.
62. Gridley T. Notch signaling in the vasculature. *Curr Top Dev Biol* 2010; 92: 277–309.
63. Yamamura H, Yamamura A, Ko EA, et al. Activation of Notch signaling by short-term treatment with Jagged-1 enhances store-operated Ca^{2+} entry in human pulmonary arterial smooth muscle cells. *Am J Physiol Cell Physiol* 2014; 306: C871–C878.
64. Chipperfield AR and Harper AA. Chloride in smooth muscle. *Prog Biophys Mol Biol* 2000; 74: 175–221.
65. Kitamura K and Yamazaki J. Chloride channels and their functional roles in smooth muscle tone in the vasculature. *Jpn J Pharmacol* 2001; 85: 351–357.
66. Makino A, Firth AL and Yuan JX. Endothelial and smooth muscle cell ion channels in pulmonary vasoconstriction and vascular remodeling. *Compr Physiol* 2011; 1: 1555–1602.
67. Sun H, Paudel O and Sham JS. Altered expression of chloride transporters in rat pulmonary arterial smooth muscle associated with chronic hypoxic pulmonary hypertension. *Circulation* 2014; 130: A17752.
68. Zhao Y, Zhenxiang Z, Yongjian X, et al. Relationship of intracellular free Ca^{2+} concentration and calcium-activated chloride channels of pulmonary artery smooth muscle cells in rats under hypoxic conditions. *J Huazhong Univ Sci Technolog Med Sci* 2006; 26: 172–174.
69. Petousi N, Croft QP, Cavalleri GL, et al. Tibetans living at sea level have a hyporesponsive hypoxia-inducible factor system and blunted physiological responses to hypoxia. *J Appl Physiol* 2014; 116: 893–904.
70. Karamsetty VS, MacLean MR, McCulloch KM, et al. Hypoxic constrictor response in the isolated pulmonary artery from chronically hypoxic rats. *Respir Physiol* 1996; 105: 85–93.
71. Kim HJ and Yoo HY. Hypoxic pulmonary vasoconstriction and vascular contractility in monocrotaline-induced pulmonary arterial hypertensive rats. *Korean J Physiol Pharmacol* 2016; 20: 641–647.
72. McMurtry IF, Petrun MD and Reeves JT. Lungs from chronically hypoxic rats have decreased pressor response to acute hypoxia. *Am J Physiol Heart Circ Physiol* 1978; 235: H104–H109.
73. McDaniel SS, Platoshyn O, Wang J, et al. Capacitative Ca^{2+} entry in agonist-induced pulmonary vasoconstriction. *Am J Physiol Lung Cell Mol Physiol* 2001; 280: L870–L880.
74. Wang J, Shimoda LA, Weigand L, et al. Acute hypoxia increases intracellular $[Ca^{2+}]$ in pulmonary arterial smooth muscle by enhancing capacitative Ca^{2+} entry. *Am J Physiol Lung Cell Mol Physiol* 2005; 288: L1059–L1069.
75. Wang J, Weigand L, Lu W, et al. Hypoxia inducible factor 1 mediates hypoxia-induced TRPC expression and elevated intracellular Ca^{2+} in pulmonary arterial smooth muscle cells. *Circ Res* 2006; 98: 1528–1537.
76. Platoshyn O, Brevnova EE, Burg ED, et al. Acute hypoxia selectively inhibits KCNA5 channels in pulmonary artery smooth muscle cells. *Am J Physiol Cell Physiol* 2006; 290: C907–C916.
77. Mauban JR, Remillard CV and Yuan JX. Hypoxic pulmonary vasoconstriction: role of ion channels. *J Appl Physiol (1985)* 2005; 98: 415–420.
78. Yuan XJ, Goldman WF, Tod ML, et al. Hypoxia reduces potassium currents in cultured rat pulmonary but not mesenteric arterial myocytes. *Am J Physiol* 1993; 264: L116–L123.
79. Archer SL, Wu XC, Thebaud B, et al. Preferential expression and function of voltage-gated, O_2-sensitive K^+ channels in resistance pulmonary arteries explains regional heterogeneity in hypoxic pulmonary vasoconstriction: ionic diversity in smooth muscle cells. *Circ Res* 2004; 95: 308–318.
80. Lopez-Barneo J, Lopez-Lopez JR, Urena J, et al. Chemotransduction in the carotid body: K^+ current modulated by PO_2 in type I chemoreceptor cells. *Science* 1988; 241: 580–582.
81. Perez-Reyes E. Molecular physiology of low-voltage-activated t-type calcium channels. *Physiol Rev* 2003; 83: 117–161.
82. Wang F, Koide M and Wellman GC. Nifedipine inhibition of high-voltage activated calcium channel currents in cerebral artery myocytes is influenced by extracellular divalent cations. *Front Physiol* 2017; 8: 210.
83. Sonkusare S, Palade PT, Marsh JD, et al. Vascular calcium channels and high blood pressure: pathophysiology and therapeutic implications. *Vascul Pharmacol* 2006; 44: 131–142.
84. Asano T, Noda Y, Tanaka K-I, et al. A_{2B} adenosine receptor inhibition by the dihydropyridine calcium channel blocker nifedipine involves colonic fluid secretion. *Sci Rep* 2020; 10: 3555.

85. Chevalier M, Gilbert G, Roux E, et al. T-type calcium channels are involved in hypoxic pulmonary hypertension. *Cardiovasc Res* 2014; 103: 597–606.
86. Weissmann N, Dietrich A, Fuchs B, et al. Classical transient receptor potential channel 6 (TRPC6) is essential for hypoxic pulmonary vasoconstriction and alveolar gas exchange. *Proc Natl Acad Sci USA* 2006; 103: 19093–19098.
87. Itsuki K, Imai Y, Hase H, et al. PLC-mediated PI(4,5)P2 hydrolysis regulates activation and inactivation of TRPC6/7 channels. *J Gen Physiol* 2014; 143: 183–201.
88. Shi J, Geshi N, Takahashi S, et al. Molecular determinants for cardiovascular TRPC6 channel regulation by Ca^{2+}/calmodulin-dependent kinase II. *J Physiol* 2013; 591: 2851–2866.
89. Takahashi S, Lin H, Geshi N, et al. Nitric oxide-cGMP-protein kinase G pathway negatively regulates vascular transient receptor potential channel TRPC6. *J Physiol* 2008; 586: 4209–4223.
90. Smith KA, Ayon RJ, Tang H, et al. Calcium-sensing receptor regulates cytosolic [Ca^{2+}] and plays a major role in the development of pulmonary hypertension. *Front Physiol* 2016; 7: 517.
91. Merritt JE, Armstrong WP, Benham CD, et al. SKF 96365, a novel inhibitor of receptor-mediated calcium entry. *Biochem J* 1990; 271: 515–522.
92. Singh A, Hildebrand ME, Garcia E, et al. The transient receptor potential channel antagonist SKF96365 is a potent blocker of low-voltage-activated T-type calcium channels. *Br J Pharmacol* 2010; 160: 1464–1475.
93. Lin BL, Matera D, Doerner JF, et al. In vivo selective inhibition of TRPC6 by antagonist BI 749327 ameliorates fibrosis and dysfunction in cardiac and renal disease. *Proc Natl Acad Sci USA* 2019; 116: 10156–10161.
94. Xia Y, Fu Z, Hu J, et al. TRPV4 channel contributes to serotonin-induced pulmonary vasoconstriction and the enhanced vascular reactivity in chronic hypoxic pulmonary hypertension. *Am J Physiol Cell Physiol* 2013; 305: C704–C715.
95. Moran MM, McAlexander MA, Bíró T, et al. Transient receptor potential channels as therapeutic targets. *Nature Rev Drug Discov* 2011; 10: 601–620.
96. Brown EM and MacLeod RJ. Extracellular calcium sensing and extracellular calcium signaling. *Physiol Rev* 2001; 81: 239–297.
97. Hofer AM and Brown EM. Extracellular calcium sensing and signalling. Nat Rev Mol Cell *Biol* 2003; 4: 530–538.
98. Magno AL, Ward BK and Ratajczak T. The calcium-sensing receptor: a molecular perspective. *Endocr Rev* 2011; 32: 3–30.
99. Ju M, Shi J, Saleh SN, et al. Ins(1,4,5)P3 interacts with PIP2 to regulate activation of TRPC6/C7 channels by diacylglycerol in native vascular myocytes. *J Physiol* 2010; 588: 1419–1433.
100. Song S, Babicheva A, Zhao T, et al. Notch enhances Ca^{2+} entry by activating calcium-sensing receptors and inhibiting voltage-gated K^+ channels. *Am J Physiol Cell Physiol* 2020; 318: C954–C968.
101. Wang Y-C, Chen Q, Luo J-M, et al. Notch1 promotes the pericyte-myofibroblast transition in idiopathic pulmonary fibrosis through the PDGFR/ROCK1 signal pathway. *Exp Mol Med* 2019; 51: 1–11.
102. Leblanc N, Forrest AS, Ayon RJ, et al. Molecular and functional significance of Ca^{2+}-activated Cl^- channels in pulmonary arterial smooth muscle. *Pulm Circ* 2015; 5: 244–268.
103. Large WA and Wang Q. Characteristics and physiological role of the Ca^{2+}-activated Cl^- conductance in smooth muscle. *Am J Physiol* 1996; 271: C435–C454.
104. Hartzell C, Putzier I and Arreola J. Calcium-activated chloride channels. *Annu Rev Physiol* 2005; 67: 719–758.
105. Caputo A, Caci E, Ferrera L, et al. TMEM16A, a membrane protein associated with calcium-dependent chloride channel activity. *Science* 2008; 322: 590–594.
106. Sun H, Xia Y, Paudel O, et al. Chronic hypoxia-induced upregulation of Ca^{2+}-activated Cl^- channel in pulmonary arterial myocytes: a mechanism contributing to enhanced vasoreactivity. *J Physiol* 2012; 590: 3507–3521.
107. Forrest AS, Joyce TC, Huebner ML, et al. Increased TMEM16A-encoded calcium-activated chloride channel activity is associated with pulmonary hypertension. *Am J Physiol Cell Physiol* 2012; 303: C1229–C1243.
108. Boedtkjer DMB, Kim S, Jensen AB, et al. New selective inhibitors of calcium-activated chloride channels – T16Ainh-A01, CaCCinh-A01 and MONNA – what do they inhibit? *Br J Pharmacol* 2015; 172: 4158–4172.
109. Papp R, Nagaraj C, Zabini D, et al. Targeting TMEM16A to reverse vasoconstriction and remodelling in idiopathic pulmonary arterial hypertension. *Eur Respir J* 2019; 53: 1800965.
110. Procianoy E, De Abreu ESFA, Marostica PJC, et al. Chloride conductance, nasal potential difference and cystic fibrosis pathophysiology. *Lung* 2020; 198: 151–156.
111. Shamsuddin AKM and Quinton PM. Concurrent absorption and secretion of airway surface liquids and bicarbonate secretion in human bronchioles. *Am J Physiol Lung Cell Mol Physiol* 2019; 316: L953–L960.
112. Tabeling C, Yu H, Wang L, et al. CFTR and sphingolipids mediate hypoxic pulmonary vasoconstriction. *Proc Natl Acad Sci U S A* 2015; 112: E1614–E1623.
113. Robertson TP, Dipp M, Ward JP, et al. Inhibition of sustained hypoxic vasoconstriction by Y-27632 in isolated intrapulmonary arteries and perfused lung of the rat. *Br J Pharmacol* 2000; 131: 5–9.
114. Takemoto M, Sun J, Hiroki J, et al. Rho-kinase mediates hypoxia-induced downregulation of endothelial nitric oxide synthase. *Circulation* 2002; 106: 57–62.
115. Fagan KA, Oka M, Bauer NR, et al. Attenuation of acute hypoxic pulmonary vasoconstriction and hypoxic pulmonary hypertension in mice by inhibition of Rho-kinase. *Am J Physiol Lung Cell Mol Physiol* 2004; 287: L656–L664.
116. Hopkins N and McLoughlin P. The structural basis of pulmonary hypertension in chronic lung disease: remodelling, rarefaction or angiogenesis? *J Anat* 2002; 201: 335–348.
117. Penaloza D and Arias-Stella J. The heart and pulmonary circulation at high altitudes: healthy highlanders and chronic mountain sickness. *Circulation* 2007; 115: 1132–1146.
118. Wang J, Weigand L, Wang W, et al. Chronic hypoxia inhibits Kv channel gene expression in rat distal pulmonary artery. *Am J Physiol Lung Cell Mol Physiol* 2005; 288: L1049–L1058.
119. Lin M-J, Leung GPH, Zhang W-M, et al. Chronic hypoxia induced upregulation of store-operated and receptor-operated Ca^{2+} channels in pulmonary arterial smooth muscle cells. *Circ Res* 2004; 95: 496–505.
120. Waypa GB, Marks JD, Guzy RD, et al. Superoxide generated at mitochondrial complex III triggers acute responses to hypoxia in the pulmonary circulation. *Am J Respir Crit Care Med* 2013; 187: 424–432.

121. Schumacker PT. Lung cell hypoxia: role of mitochondrial reactive oxygen species signaling in triggering responses. *Proc Am Thorac Soc* 2011; 8: 477–484.
122. Waypa GB, Guzy R, Mungai PT, et al. Increases in mitochondrial reactive oxygen species trigger hypoxia-induced calcium responses in pulmonary artery smooth muscle cells. *Circ Res* 2006; 99: 970–978.
123. Michelakis ED, McMurtry MS, Wu X-C, et al. Dichloroacetate, a metabolic modulator, prevents and reverses chronic hypoxic pulmonary hypertension in rats. *Circulation* 2002; 105: 244–250.
124. Reeve HL, Michelakis E, Nelson DP, et al. Alterations in a redox oxygen sensing mechanism in chronic hypoxia. *J Appl Physiol* 2001; 90: 2249–2256.
125. Broughton BR, Jernigan NL, Norton CE, et al. Chronic hypoxia augments depolarization-induced Ca^{2+} sensitization in pulmonary vascular smooth muscle through superoxide-dependent stimulation of RhoA. *Am J Physiol Lung Cell Mol Physiol* 2010; 298: L232–L242.
126. Leach RM, Robertson TP, Twort CH, et al. Hypoxic vasoconstriction in rat pulmonary and mesenteric arteries. *Am J Physiol* 1994; 266: L223–L231.
127. Weissmann N, Akkayagil E, Quanz K, et al. Basic features of hypoxic pulmonary vasoconstriction in mice. *Respir Physiol Neurobiol* 2004; 139: 191–202.
128. Rhoades RA. Isolated perfused lung preparation for studying altered gaseous environments. *Environ Health Perspect* 1984; 56: 43–50.
129. Deng Y, Rowe KJ, Chaudhary KR, et al. Optimizing imaging of the rat pulmonary microvasculature by micro-computed tomography. *Pulm Circ* 2019; 9: 2045894019883613.